ADVANCED SULFUR CONTROL CONCEPTS IN HOT-GAS DESULFURIZATION TECHNOLOGY: PHASE 2. EXPLORATORY STUDIES ON THE DIRECT PRODUCTION OF ELEMENTAL SULFUR DURING THE REGENERATION OF HIGH TEMPERATURE DESULFURIZATION SORBENTS

Topical Report

A. Lopez
W. Huang
J. White
Y. Zeng
F.R. Groves
D.P. Harrison

July 1997

Work Performed Under Contract No.: DE-AC21-94MC30012--13

for
Federal Energy Technology Center
Morgantown, West Virginia

by
Louisiana State University
Department of Chemical Engineering
Baton Rouge, Louisiana

DISCLAIMER

DISCLAIMER

Portions of this document may be illegible electronic image products. Images are produced from the best available original document.

ACKNOWLEDGMENT

This research is sponsored by the U.S. Department of Energy, Federal Energy Technology Center under contract number DE-AC21-94MC30012. The authors are particularly grateful for the assistance and advice provided by Mr. Thomas Dorchak of FETC.

EXECUTIVE SUMMARY

The topical report describes the results of Phase 2 research to determine the feasibility of the direct production of elemental sulfur during the regeneration of high temperature desulfurization sorbents. Results of Phase 1 research, which included a literature survey and thermodynamic analysis of elemental sulfur production, were presented in an earlier topical report dated October 1994.

The Federal Energy Technology Center - Morgantown of the U.S. Department of Energy has primary responsibility for the development of advanced power systems to enable the nation's vast coal reserves to be used in an economical and environmentally acceptable manner. Integrated gasification combined cycle (IGCC) technology has emerged as a major thrust in meeting this responsibility. IGCC power plants are attractive because of their low emissions and increased electrical generation efficiency.

Many of the contaminants present in coal emerge from the gasification process in the product gas. The contaminants, in the form of H_2S, NH_3, halogens, etc., must be removed prior to power generation. Using current technology, these contaminants can only be removed at low temperature. This requires that the coal gas be cooled, treated, and reheated prior to power generation. The purification process would be simplified and the overall thermodynamic efficiency increased if the contaminants could be removed at high temperature.

Much effort has gone into the development of high temperature metal oxide sorbents for removal of H_2S from coal gas. The oxides of zinc, iron, manganese, and others have been studied. In order for high temperature desulfurization to be economical it is necessary that the sorbents be regenerated to permit multicycle operation. Current methods of sorbent regeneration involve oxidation of the metal sulfide to reform the metal oxide and free the sulfur as SO_2. There are a number of problems associated with this method of regeneration. The oxidation reaction is highly exothermic, which complicates the problem of regeneration reactor temperature control and may hasten sorbent deterioration through sintering. Limiting regenerator temperature excursions may be accomplished by diluting the oxygen in the regeneration feed gas. This approach reduces the SO_2 concentration in the regeneration product gas and complicates the ultimate SO_2 control problem. Finally, the sulfates of many of the candidate sorbents may be formed in the SO_2 - O_2 atmosphere. Spalling caused by the formation of the $ZnSO_4$ is one of the problems which has delayed the development of zinc-based sorbent processes.

An alternate regeneration process in which the sulfur is liberated in elemental form is desired. Elemental sulfur, which is the typical feed to sulfuric acid plants, may be easily separated, stored, and transported. Although research to convert SO_2 produced during sorbent regeneration to elemental sulfur is on-going, additional processing steps are required and the overall process will be more complex. Clearly, the direct production of elemental sulfur is preferred.

This study began with a literature search to identify possible concepts for elemental sulfur production during regeneration and to gather relevant thermodynamic, kinetic, and process data. Following the literature search, a thermodynamic analysis, based on free energy minimization, was carried out to evaluate candidate sorbents for possible use with the regeneration concepts. As a result of this effort, iron- and cerium-based sorbents were selected for the preliminary experimental study.

Neither of these materials possesses the high H_2S removal capability associated with zinc-based sorbents. However, on the basis of the thermodynamic analysis, both are more likely to produce elemental sulfur during the regeneration phase.

The regeneration of FeS has been investigated using the so-called partial oxidation concept in which the regeneration feed gas contains large H_2O/O_2 ratios. Electrobalance reactor studies were performed initially to obtain comparative kinetics of the FeS-O_2 and FeS-H_2O reactions. This was followed by a series of laboratory-scale fixed-bed reactor tests in which the distribution of sulfur species in the regeneration product gas was determined as a function of reaction time. Real time product gas analysis required the development of a new analytical method for simultaneous measurement of SO_2, H_2S, and elemental sulfur concentrations. Large portions of the sulfur originally present in FeS were liberated in elemental form. For example, instantaneous and cumulative elemental sulfur selectivities of greater than 80% and about 75% of theoretical, respectively, were measured. However, the large H_2O/O_2 ratio meant that the elemental sulfur concentration in the product gas was quite small. The large steam requirement was judged to render the process uneconomical.

The thermodynamic properties of Ce_2O_2S, the sulfided form of CeO_2, are unique in that regeneration to elemental sulfur is favored using each of the three regeneration concepts identified in the literature search. The most favorable concept is based on regeneration with SO_2 which is represented by the following reaction:

$$Ce_2O_2S(s) + SO_2(g) ==> 2CeO_2(s) + S_2(g)$$

This concept is basically free of side reactions, and the thermodynamics permit complete Ce_2O_2S regeneration at 1000 K and 25 atm with less than 30% excess SO_2. Under these conditions, the regeneration product gas would contain about 85% elemental sulfur.

In contrast to zinc-based sorbents, problems associated with CeO_2 are associated primarily with the desulfurization step. CeO_2 is not thermodynamically capable of reducing H_2S concentrations to the 20 ppmv target level. Therefore, a two-stage process in which CeO_2 would be used for bulk H_2S removal, and a zinc-based sorbent would be used for H_2S polishing has been proposed. Elemental sulfur is to be produced directly during Ce_2O_2S regeneration while the relatively small quantity of ZnS is to be regenerated in the traditional manner using O_2 with the SO_2 recycled to the gasifier.

Preliminary tests involving the sulfidation of CeO_2 to Ce_2O_2S and regeneration back to CeO_2 by reaction with SO_2 have been carried out in the fixed-bed reactor. Preparation of Ce_2O_2S by sulfidation of CeO_2 is necessary since Ce_2O_2S cannot be obtained commercially. Also, all cerium sorbent testing has been limited to the fixed-bed reactor; there is no change in solid mass involved in the conversion of $2CeO_2$ to Ce_2O_2S so that no information can be gained from electrobalance reactor tests.

During sulfidation at 800°C, the H_2S concentration during the prebreakthrough period has been reduced from 10,000 ppmv in the feed gas to 100 ppmv (or less) in the product gas. The

thermal conductivity detector used for H_2S analysis is limited to approximately 100 ppmv. While there are indications that prebreakthrough H_2S concentrations in the range of 20 to 40 ppmv have been achieved, the results at this concentration level are uncertain.

Quite favorable results have been obtained from tests involving the regeneration of Ce_2O_2S with SO_2. At 600°C, the reaction is rapid and goes to completion. The SO_2 content of the regeneration feed gas has been as high at 12 mol %, and the elemental sulfur content of the product gas (measured as S_2) has approached 12% prior to SO_2 breakthrough. Ten complete sulfidation-regeneration cycles have been completed at the above conditions with no apparent deterioration in sorbent performance.

Favorable results from the experimental tests and on-going process analysis suggest that a desulfurization process using CeO_2-based sorbent is feasible. Additional experimental tests will be conducted during the remaining portion of the study to examine the effect of reaction conditions on both the sulfidation and regeneration performance.

Table of Contents

List of Figures

List of Tables

INTRODUCTION

The integrated gasification combined cycle (IGCC) process, which combines coal gasification with electric power generation, creates the possibility of utilizing the nation's large coal reserves with greater efficiency and less environmental impact than the current pulverized coal-steam cycle. Efficiencies of approximately 50% are possible for an optimized IGCC process. The optimized process requires that a number of contaminants be removed from the high temperature coal gas prior to power generation. Control of particulate matter and a number of gaseous materials including sulfur compounds (primarily H_2S) is required. The sulfur compounds, which constitute the primary emphasis of this study, must be removed both to meet environmental standards and to prevent corrosion of the turbine blades.

Various liquid scrubbing processes, many utilizing an amine solvent, are available for H_2S removal. However, such processes do not integrate well with the gasification and power generation sections of the IGCC process. Hot coal gases must be cooled to near ambient temperature, scrubbed, and then reheated prior to entering the power generation section. Energy losses, which reduce the efficiency of electricity generation, and gas-to-gas heat exchangers, which are necessarily large and expensive, are the inevitable result of liquid scrubbing processes for H_2S removal.

High temperature desulfurization based on the noncatalytic reaction of H_2S with an appropriate metal oxide sorbent can eliminate many of the problems associated with low temperature sulfur removal and allow the IGCC process to operate at higher efficiency. The general high temperature desulfurization reaction may be represented by

$$MeO(s) + H_2S(g) ==> MeS(s) + H_2O(g) \qquad (1)$$

Metal oxide sorbents having high sulfur capacity and the capability of reducing the H_2S content of the coal gas to about 10 ppmv are available. However, economic considerations require that the sorbent be regenerable and able to withstand many sulfidation-regeneration cycles. For these reasons the sorbent must process good mechanical strength and be resistant to attrition and sintering at the temperatures of interest.

The regeneration reaction which has received the most attention in the past involves direct oxidation of both the metal and sulfur species. This reaction is represented generically by

$$MeS(s) + 1.5O_2(g) ==> MeO(s) + SO_2(g) \qquad (2)$$

Metal sulfate formation is often favored at lower temperatures, requiring the regeneration reaction to be carried out above the sulfate decomposition temperature. Reaction (2) is highly exothermic, leading to complex reactor temperature control problems and the possibility of sorbent deterioration due to sintering. In order to control the temperature, the regeneration feed gas may contain large concentrations of inert diluent. This results in small concentrations of SO_2 in the regeneration product gas and complicates the ultimate SO_2 control problem.

These regeneration problems would be eliminated, or at least greatly alleviated, if elemental sulfur instead of SO_2 could be produced during sorbent regeneration. Partial oxidation is less

exothermic so that reactor temperature control problems would be eased. Sulfate formation can be avoided, and, most importantly, elemental sulfur can be easily separated by condensation. Liquid or solid elemental sulfur product can be stored and transported relatively easily, and, as the standard feed to sulfuric acid plants, it has commercial value.

The initial phase of this project consisted of a literature review to identify concepts for the direct production of elemental sulfur. Three concepts were identified. The first, which we refer to as partial oxidation, involves reaction of the metal sulfide in an H_2O/O_2 atmosphere operated in an O_2-starved manner. While a number of simultaneous reactions occur, the net result can be represented by

$$MeS(s) + 0.5O_2(g) ==> MeO(s) + 0.5S_2(g) \quad (3)$$

The second concept involves the use of SO_2 as the oxidant according to the following stoichiometry

$$MeS(s) + 0.5SO_2(g) ==> MeO(s) + 0.75S_2(g) \quad (4)$$

The third concept represents a direct reversal of the sulfidation reaction by reacting the metal sulfide with steam

$$MeS(s) + H_2O(g) ==> MeO(s) + H_2S(g) \quad (5)$$

Although H_2S rather than elemental sulfur is the reaction product, the concept was judged to be of interest if sufficiently high concentrations of H_2S could be produced to permit the regeneration product to be fed to a Claus reactor for elemental sulfur recovery.

In the second phase of the project, the thermodynamics of the regeneration concepts were examined using a number of candidate sorbents. In general, we concluded that sorbents having the greatest affinity for H_2S in the sulfidation phase were least amenable to the liberation of elemental sulfur during regeneration. There appeared to be little, if any, opportunity to produce elemental sulfur during the regeneration of ZnS. Iron-based sorbents are less efficient than zinc sorbents in removing H_2S and, therefore, are somewhat more amenable to the liberation of elemental sulfur. In particular, the partial oxidation regeneration of FeS was judged to be of potential interest. This conclusion was based on previous literature results as well as from the thermodynamic analysis. Successful partial oxidation regeneration would operate under kinetic, rather than thermodynamic, control.

The thermodynamic properties of sorbents based on the oxides of tin and cerium were found to be unique in terms of H_2S removal and the potential for elemental sulfur production during regeneration. While these oxides were thermodynamically less effective for H_2S removal, elemental sulfur production was favored using each of the three regeneration concepts.

The iron and cerium sorbent systems were subsequently selected for the preliminary study, and results of these preliminary tests are described in this report. FeS regeneration has been studied using the partial oxidation concept in both electrobalance and fixed-bed reactors. Since sulfidation of iron oxide has been studied extensively, the experimental activity was limited to the regeneration

of FeS obtained from commercial sources. Cerium oxysulfide, Ce_2O_2S, is the product of the reaction between CeO_2 and H_2S. Since Ce_2O_2S is not available commercially, both sulfidation and regeneration experiments were conducted. Regeneration tests used the reaction of Ce_2O_2S with SO_2. Also, since there is no solid weight change in the conversion of $2CeO_2$ to Ce_2O_2S, the electrobalance reactor was not applicable. All experimental tests used a laboratory-scale fixed-bed reactor and the progress of the reaction was monitored by analyzing the composition of the product gas as a function of time.

FeS PARTIAL OXIDATION

The electrobalance reactor was used to study the individual reactions of FeS with O_2 and with H_2O from 600 to 800°C and from 1 to 15 atm. The gas composition ranged from 0.5 to 3.0% O_2 in N_2 and from 10 to 40% H_2O in N_2. A limited number of tests were conducted using O_2-H_2O-N_2 mixtures with the H_2O content fixed at 30% and the O_2 content varied from 0.05 to 0.5%. While a number of simultaneous reactions may occur, the experimental results can be interpreted on the basis of four primary reactions:

$$2FeS(s) + 3.5O_2(g) ==> Fe_2O_3(s) + 2SO_2(g) \quad (6)$$

$$3FeS(s) + 4H_2O(g) ==> Fe_3O_4(s) + 3H_2O(g) + H_2(g) \quad (7)$$

$$2H_2S(g) + SO_2(g) ==> 2H_2O(g) + 1.5S_2(g) \quad (8)$$

$$2Fe_3O_4(s) + 0.5O_2(g) ==> 3Fe_2O_3(s) \quad (9)$$

Only reaction (6) occurs in the O_2-N_2 atmosphere, while only reaction (7) occurs in H_2O-N_2. The Claus reaction (8) is believed to be primarily responsible for elemental sulfur formation, while Fe_3O_4(s) formed by reaction (7) is rapidly oxidized to Fe_2O_3(s) by reaction (9) when contacted by O_2. Elemental sulfur is represented in reaction (8) and elsewhere as S_2(g) for convenience. In reality, various quantifies of gaseous sulfur allotropes, S_n with $8 \geq n \geq 1$, may be formed, depending on temperature and pressure.

In the electrobalance, the progress of the individual reactions (6) and (7) was followed by monitoring the change in solid mass which accompanied the conversion of FeS to either Fe_2O_3 or Fe_3O_4. The electrobalance reactor is of limited use when simultaneous gas-solid reactions occur and provides no information on gas phase reactions. Hence, the fixed-bed reactor with product gas analysis was used in most experiments when the feed gas contained both O_2 and H_2O. Fixed-bed tests were conducted at 4.4 atm over a temperature range of 550 to 700 °C. The feed gas contained 0 to 1.5% O_2, 0 to 52% H_2O and balance N_2. The H_2O/O_2 ratio in the feed gas varied from 0 to 200. Development of an analytical method to determine the concentration of sulfur species -- SO_2, H_2S, and S_2 -- as a function of time required a major effort. The method is described in a subsequent section.

Approximately 3 mg of FeS from Johnson Matthey Co. were used in the electrobalance tests. The composition and selected properties of this material, as supplied by Johnson Matthey and as

measured at LSU, are presented in the top section of Table 1. The FeS used in the fixed-bed tests was from Strem Chemicals; composition and selected properties are found in the bottom section of Table 1. From 0.5 to 3.3 g of FeS were mixed with approximately three grams of Al_2O_3 in the fixed-bed reactor runs. The quantity of FeS depended on the flow rate and O_2 content of the regeneration feed gas and was adjusted so that the reaction could be completed in a reasonable time period. Selected properties of the Al_2O_3, which was added to minimize sintering, are also found in Table 1.

Table 1. FeS Composition and Properties

Electrobalance Tests	
FeS Source	Johnson Matthey
Composition (Mass%)	
Fe	61.78
Al	<0.01
Ca	<0.01
Co	<0.01
Cu	0.02
Mg	<0.01
Mn	<0.01
Ni	<0.01
Particle Size Range	< 100 mesh
Specific Surface Area	5.3 m^2/g (Measured by LSU)
Fixed-Bed Tests	
FeS Source	Strem Chemicals
FeS Content	99.2 $\pm$ 0.1%
Particle Size Range	60 to 200 mesh
Al_2O_3 Source	Sigma Chemicals
Particle Size Range	80 to 200 mesh

Electrobalance Studies

Equipment: A schematic diagram of the high pressure electrobalance reactor system is shown in Figure 1. The electrobalance housing and reactor hangdown tube were constructed of 316 stainless steel capable of operating at 1500 psi at 600°C. The inner surface of the hangdown tube was Alonized to minimize interaction between H_2S and metal. The FeS was held in a platium pan and suspended from the electrobalance with a nichrome wire.

Ultra high purity (UHP) N_2 was fed through the electrobalance housing to prevent back diffusion of reactive gases into the balance chamber. Additional UHP N_2, air, and/or steam were fed through an opening in the side of the hangdown tube. Combined gases flowed downward over the sorbent. Gases were obtained from high-pressure cylinders and flow rate was controlled using mass flow controllers. Steam was generated by supplying water from a high pressure syringe pump. Lines were heat traced to vaporize the water and preheat the feed gas. Valves in the sidearm permitted

flow rates to be established and diverted to vent while desired reaction conditions were achieved in inert N_2. Reactor product gases passed through a condenser and were vented through a back pressure regulator. During the test the sample weight was continuously monitored and the data was stored for further processing in the data acquisition system.

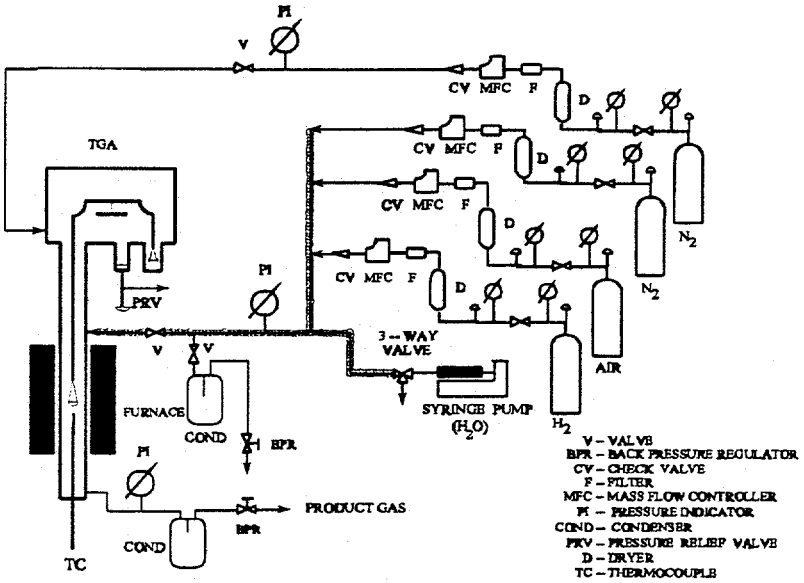

Figure 1. High Pressure Electrobalance Schematic

The raw data from the electrobalance is affected by aerodynamic drag and because of a time delay between switching the side-arm valve and the reactive gases contacting the sorbent. Delay time corrections, which depend on system volume between the side-arm valve and the sorbent, and flow rate, temperature, and pressure of the feed gas, were calculated on the basis of plug flow and applied to the raw data. The delay time varied from 0.12 to 2.94 minutes, depending on reaction conditions. Aerodynamic drag caused the apparent weight of the sample to be different from the true mass. Drag corrections as a function of temperature, pressure, and flow rate were experimentally determined under non-reacting conditions and also applied to the raw data.

Time-Conversion Results: Experimental time-conversion results including corrections for delay time and aerodynamic drag are shown in Figure 2 for a series of O_2 regeneration tests at 700°C, 5 atm, and 800 sccm total flow rate. Normalized sorbent mass, M/M_o, where M_o is the initial mass, is plotted versus reaction time. The horizontal dashed line at $M/M_o = 0.909$ is the theoretical value corresponding to the complete regeneration of pure FeS to Fe_2O_3. The experimental final values of M/M_o shown in Figure 2 range from 0.900 to 0.902. As will be seen, the final experimental values were generally in this range; the fact that they are smaller than theoretical is attributed primarily to impurities in the original FeS. The Figure 2 results show that the FeS-O_2 reaction is rapid at 700°C and is a strong function of O_2 concentration.

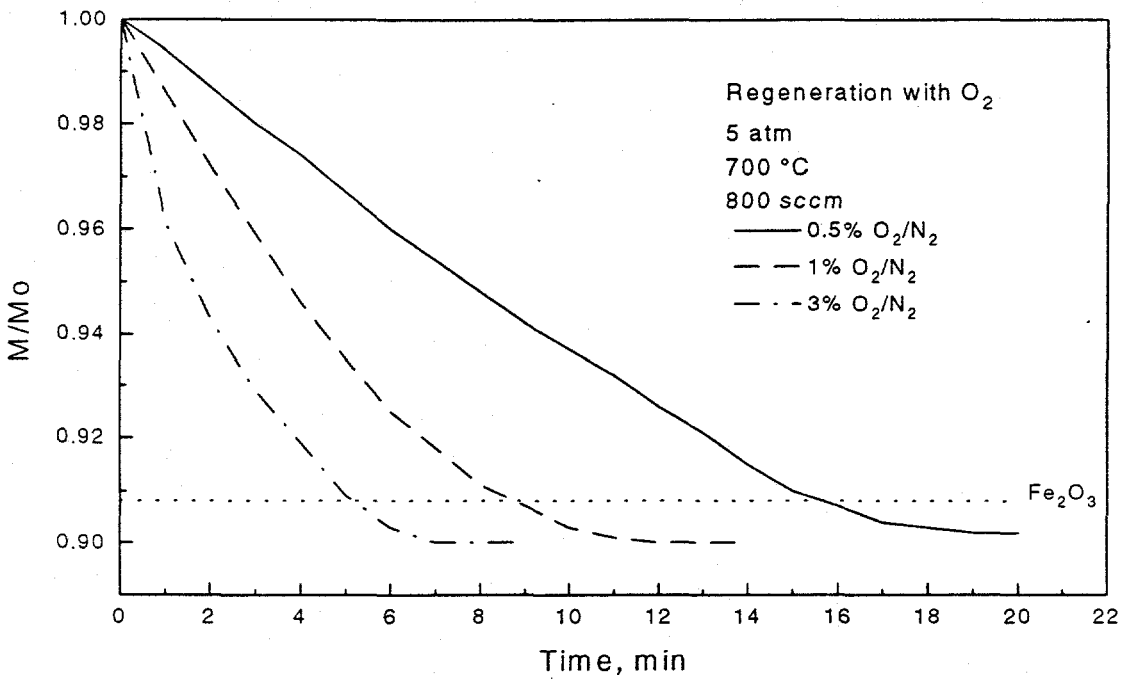

Figure 2. FeS Regeneration with O_2: The Effect of O_2 Concentration

Time-conversion results showing the effects of temperature and pressure are presented in Figures 3 and 4, respectively. In all cases the final normalized masses are slightly below theoretical. The effect of temperature, Figure 3, is shown at 5 atm using 1% O_2 at a feed gas rate of 800 sccm. The important result is the relatively small effect of temperature. Between 11 and 12 minutes were required for M/M_o to reach the theoretical value of 0.0909 at 600°C while 7 to 8 minutes were required at 800°C. The effect of pressure is shown in Figure 4 at 700°C, 1% O_2 and a flow rate of 800 sccm. A relatively small increase in rate was observed in going from 1 to 5 atm, but the rate at 15 atm was slightly smaller than the 1 atm rate. This result was surprising since the O_2 concentration increased proportionally with pressure. The results shown in Figures 2 through 4 were typical of the results obtained at other reaction conditions.

Similar results for the FeS-H_2O reaction showing the effect of H_2O concentration, temperature, and pressure on the normalized mass versus time results are shown in Figures 5, 6, and 7, respectively. The horizontal dashed line in the figures at $M/M_o = 0.878$ corresponds to the stoichiometric value associated with complete conversion of FeS to Fe_3O_4. In these tests, there was greater scatter in the final values of M/M_o, with the experimental results being both above and below the stoichiometric value.

The reaction rate is a strong function of H_2O mol fraction (Figure 5), just as the FeS-O_2 reaction. The temperature dependence of the FeS-H_2O reaction (Figure 6) is somewhat greater than for the FeS-O_2 reaction, and the same unexpected effect of pressure was observed in both reactions. Figure 7 shows that the rate of the FeS-H_2O reaction increased with pressure from 1 to 5 atm, but the rate at 15 atm was considerably smaller than the rate at 1 atm.

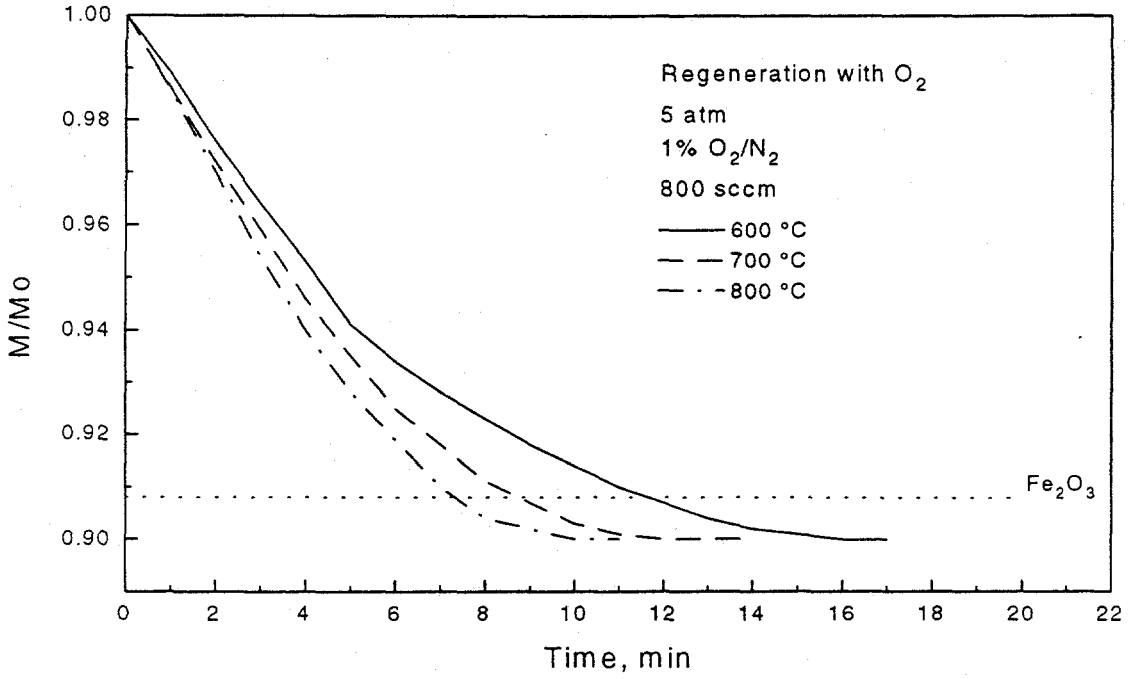

Figure 3. FeS Regeneration with O_2: The Effect of Temperature

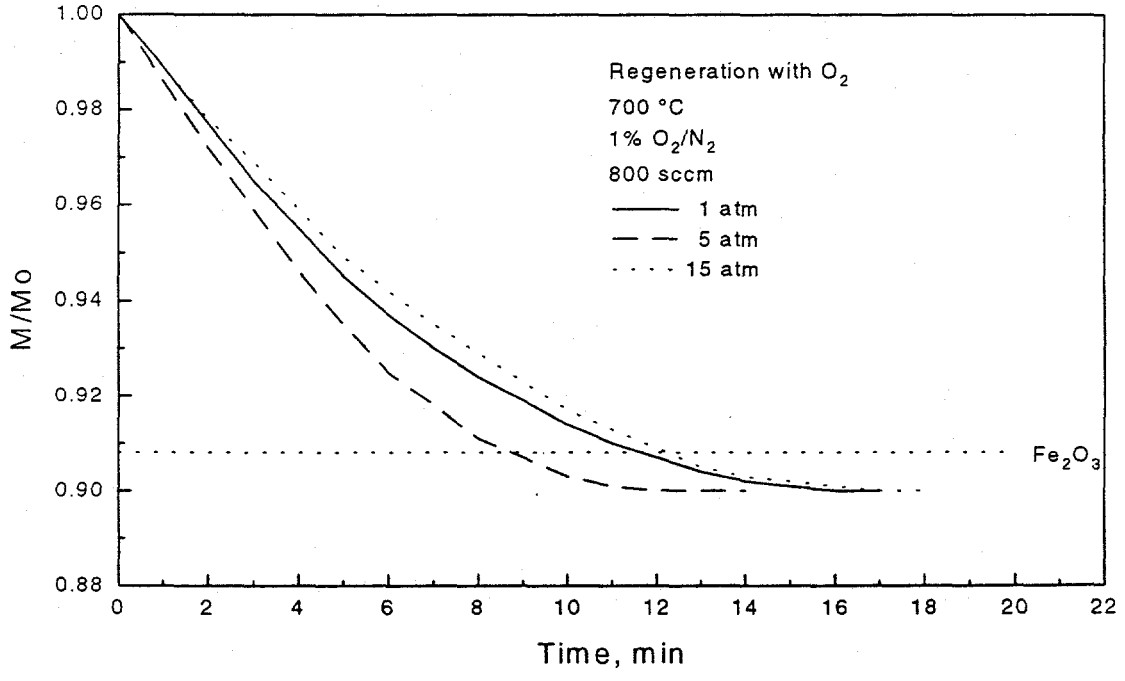

Figure 4. FeS Regeneration with O_2: The effect of Pressure

Comparison of the FeS-O_2 results (Figures 2 - 4) with the FeS-H_2O results (Figures 5- 7) shows that FeS reacts much faster with O_2 than with H_2O. For example, at 700°C and 5 atm, approximately 18 minutes were required for complete regeneration in 0.5% O_2 (Figure 2) while almost 25 minutes were required for complete regeneration in 40% H_2O at the same temperature and pressure (Figure 5).

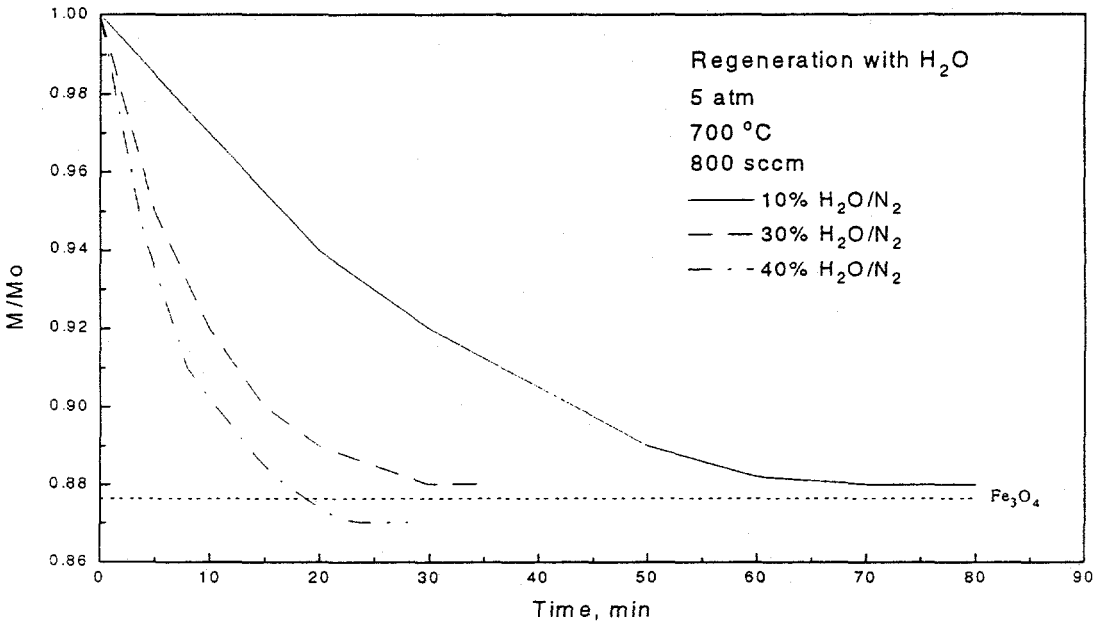

Figure 5. FeS Regeneration with H_2O: The Effect of H_2O Concentration

A limited number of electrobalance tests were carried out in which the feed gas contained both O_2 and H_2O. The H_2O content was held constant at 30% while the O_2 was varied from 0.05 to 0.5%. Normalized mass-time results as a function of O_2 content are shown in Figure 8. Horizontal dotted lines representing stoichiometric conversion to Fe_2O_3 and Fe_3O_4 are included in the figure. The final value of M/M_o in all tests was slightly less than the stoichiometric value for Fe_2O_3 and was effectively equal to the value obtained in all FeS-O_2 tests. This was expected since any Fe_3O formed by the FeS-H_2O reaction should quickly be oxidized to Fe_2O_3 in the presence of O_2 via reaction (9).

The H_2O/O_2 ratio ranged from 60 to 600 in the tests shown in Figure 8. These ratios were sufficiently large that both the FeS-O_2 and FeS-H_2O reactions contributed significantly to the total reaction rate. For example, from Figure 5 using 30% H_2O and no O_2, about 30 minutes were required for complete reaction, compared to 10 minutes for complete reaction when 0.05% O_2 was added to the same H_2O concentration (Figure 8). Similarly, from Figure 2, 18 minutes were required for complete reaction in 0.5% O_2 with no H_2O. This was reduced to the 8 minutes shown in Figure 8 when 30% H_2O was added.

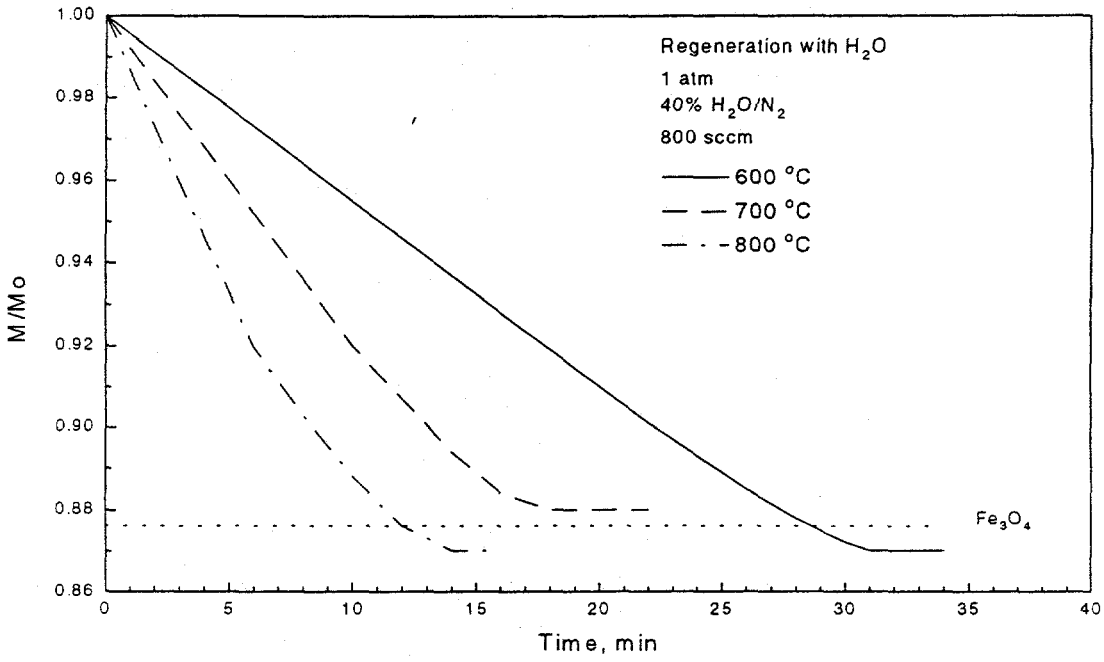

Figure 6. FeS Regeneration with H_2O: The Effect of Temperature

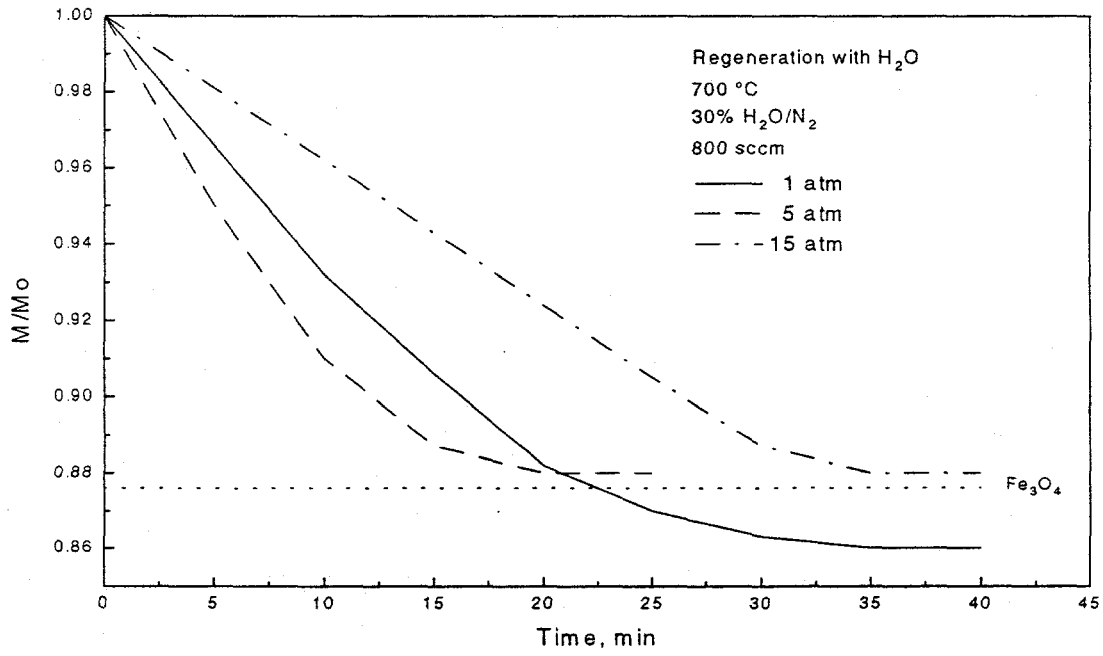

Figure 7. FeS Regeneration with H_2O: The Effect of Pressure

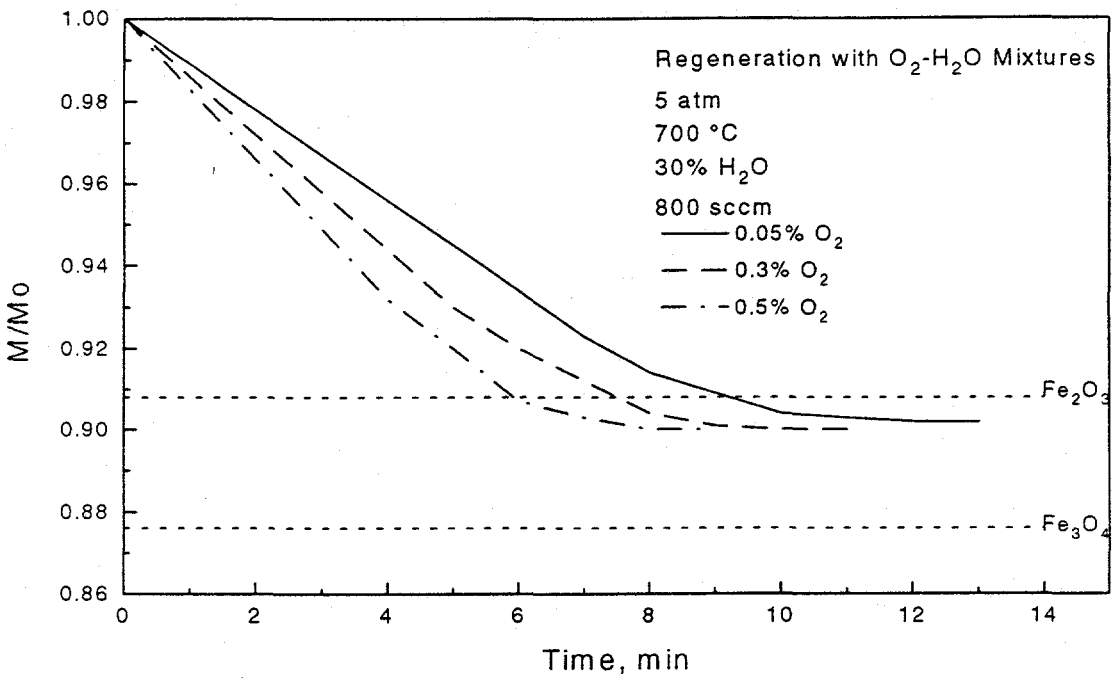

Figure 8. FeS Regeneration with O_2 and H_2O: The Effect of O_2 Concentration

The effects of temperature and pressure for the combined O_2-H_2O reactions were qualitatively similar to those observed for the single reactions. An increase in temperature between 600 and 800°C resulted in a relatively small increase in the regeneration rate. The rate increased with pressure between 1 and 5 atm, but decreased to a minimum value at 15 atm.

Fixed-Bed Reactor Studies

Equipment: A diagram of the fixed-bed reactor system is shown in Figure 9. The gas flow arrangement was similar to that used in the electrobalance reactor. Air and N_2 were obtained from high pressure cylinders and flow rates were controlled using mass flow controllers. Liquid water was fed using a high pressure syringe pump and downstream lines were heat traced to insure vaporization and to preheat the feed gases. The flow arrangement was such that N_2, O_2, and steam rates could be established and directed to vent while inert N_2 flowed through the reactor. Reactive gases were fed to the reactor by switching valve positions in the feed gas lines. The feed gases entered near the top of the reactor and flowed downward through the sorbent bed.

The sorbent was contained in an Alonized stainless steel insert within the pressure vessel. A porous quartz disc was supported on a ring welded into the insert. A layer of quartz wool was added above the disc and sorbent was placed above the quartz wool. High temperature O-rings at the top of the insert provided a seal between the insert and pressure vessel and prevented gas by-passing.

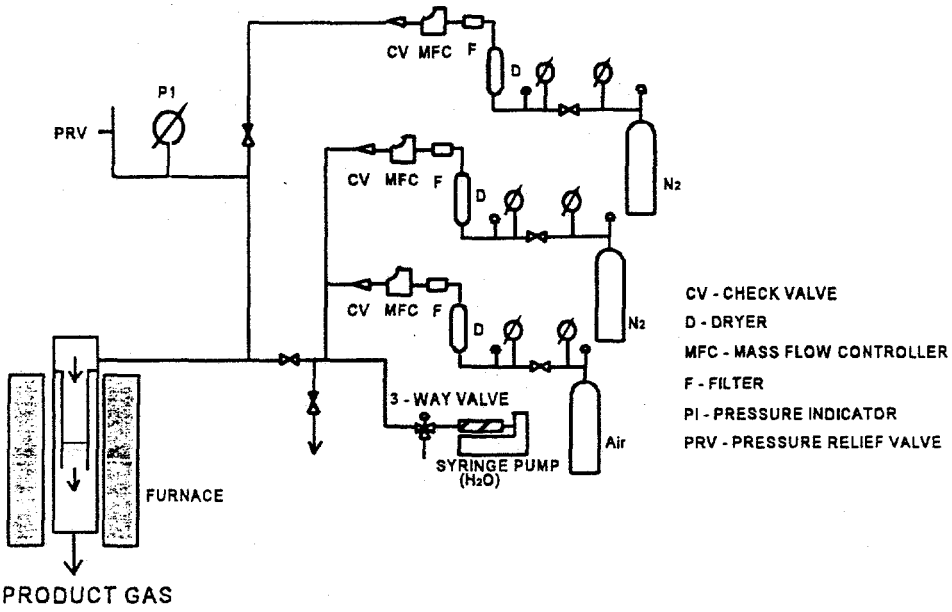

Figure 9. Fixed-Bed reactor schematic

Reactor product gases exited from the bottom of the reactor and entered the analytical system shown in Figure 10. Exit lines were maintained at high temperature to prevent elemental sulfur condensation. The product gas was split into two steams, with one portion flowing through a capillary flow restrictor into an oxidation chamber at 1050°C where all sulfur compounds were converted to SO_2. Excess H_2O was removed using a membrane dryer and total sulfur concentration was determined using a calibrated UV-Fluorescence detector. Flow through this portion of the analytical system was determined by the reactor pressure and the resistance of the capillary restrictor. As might be excepted, this system proved to be quite troublesome and frequent recalibration was necessary. The primary problem was caused by the resistance of the restrictor varying due to particulate carryover from the reactor.

The remainder of the product gas entered the bottom leg of the analytical system and passed through a condenser and series of filters where elemental sulfur was separated from the permanent gases. H_2S and SO_2 concentrations were then determined by gas chromatography. Although the technique involved the determination of elemental sulfur by difference (total sulfur- H_2S-SO_2), it provided reasonable accuracy when the concentration of elemental sulfur was sufficiently large.

Experimental Results: Reaction conditions associated with each of the experimental runs described in this report are presented in Table 2. Pressure was constant at 4.4 atm while temperature varied between 550 and 700°C. The regeneration feed gas contained from 0 to 1.5% O_2, 0 to 52% H_2O, and balance N_2. In runs in which the feed gas contained both H_2O and O_2, the H_2O/O_2 ratio ranged from 6.7 to 200. The sorbent bed consisted of a physical mixture of FeS and Al_2O_3, with the quantity of FeS varied in relation to the feed gas flow rate and O_2 content to insure complete regeneration in a reasonable time. Volumetric feed rate ranged from 300 to 600 sccm. Reaction conditions, in

particular temperature and feed gas composition, were selected on the basis of the electrobalance test results.

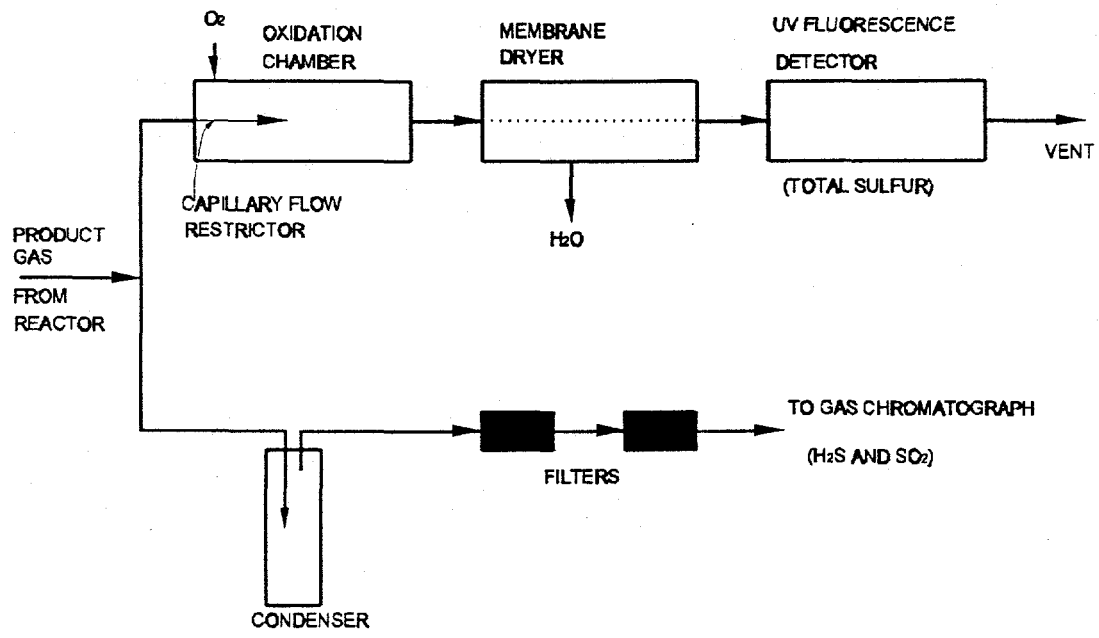

Figure 10. Product Gas Analytical System

With O_2 as the only reactive component in the feed gas, all sulfur should be liberated as SO_2 according to reaction (6). Experimental results from run FeS-11, expressed as mol fraction SO_2 in the product gas as a function of dimensionless time are shown in Figure 11. Dimensionless time is defined so that $t^* = 1$ would correspond to complete regeneration of FeS and complete conversion of O_2 if the reaction occurred at an infinitely fast rate. After a brief delay at the beginning of the run, the SO_2 concentration increased quickly to about 0.0085 mol fraction and was approximately constant until the reaction neared completion. The FeS-O_2 reaction was quite rapid as indicated by the steepness of the SO_2 concentration decrease near the end of the run, and the facts that the "steady-state" SO_2 concentration was near the stoichiometric value corresponding to complete O_2 consumption (indicated by the dashed horizontal line) and that the reaction was almost complete at $t^* = 1.0$.

When the feed gas contained only H_2O, all sulfur was liberated as H_2S according to reaction (7). In agreement with electrobalance test results, this reaction was quite slow as shown by the results of run FeS-14 in Figure 12. The steady-state H_2S concentration was only about 1.7% of the stoichiometric maximum, and regeneration was only 12% complete when the run was terminated after eight dimensionless time steps. The greater scatter in the data is attributed to the difficulty in maintaining a constant steam flow rate.

Table 2. Reaction Conditions for FeS Partial Oxidation Regeneration

Run	FeS-04	FeS-11	FeS-14	FeS-16	FeS-19	FeS-22	FeS-25	FeS-26
Sorbent Mass, g								
FeS	1.73	3.27	3.22	3.21	0.83	0.83	0.50	0.83
Al_2O_3	3.04	3.29	3.21	3.27	3.28	3.28	3.80	3.29
Temperature, °C	550	600	700	700	700	600	600	600
Pressure, atm	4.4	4.4	4.4	4.4	4.4	4.4	4.4	4.4
Feed Gas Composition, mol%								
O_2	0.5	1.5	0	1.5	0.25	0.25	0.26	0.25
H_2O	23.3	0	10.0	10.0	20.0	20.0	52.0	20.0
N_2	76.2	98.5	90.0	88.5	79.75	79.75	47.74	79.75
H_2O/O_2	47	--	--	6.7	80	80	200	80
Feed Gas Rate, sccm	300	600	600	600	300	300	435	600

When the feed gas contains both O_2 and H_2O, reactions (8) and (9) also become important. The formation of elemental sulfur by the Claus reaction depends on the relative quantities of SO_2 and H_2S and the position within the sorbent bed where they are formed. There must be sufficient H_2S-SO_2 contact time for the Claus reaction to occur.

Results from run FeS-22 in which the feed gas contained H_2O and O_2 in a 80-to-1 ratio are shown in Figure 13. The mol factions of SO_2 and H_2S determined by gas chromatography and total sulfur determined by the UV-fluorescence detector are plotted versus dimensional time. Dimensional time is used since dimensionless time cannot be clearly defined when multiple reactions occur. After a brief delay, both the total sulfur and H_2S concentrations increased rapidly with the total sulfur reaching a maximum of 0.0025 mol fraction after 0.9 hours and the H_2S maximum of 0.00065 mol fraction occurring after 1.7 hours. SO_2 concentration was effectively zero during the first hour and then gradually increased to a maximum of 0.00072 after six hours. After reaching their maxima, the concentrations of all species decreased gradually. The H_2S mol fraction approached zero after 5.1 hours and the total sulfur and SO_2 concentrations approached zero after eight hours.

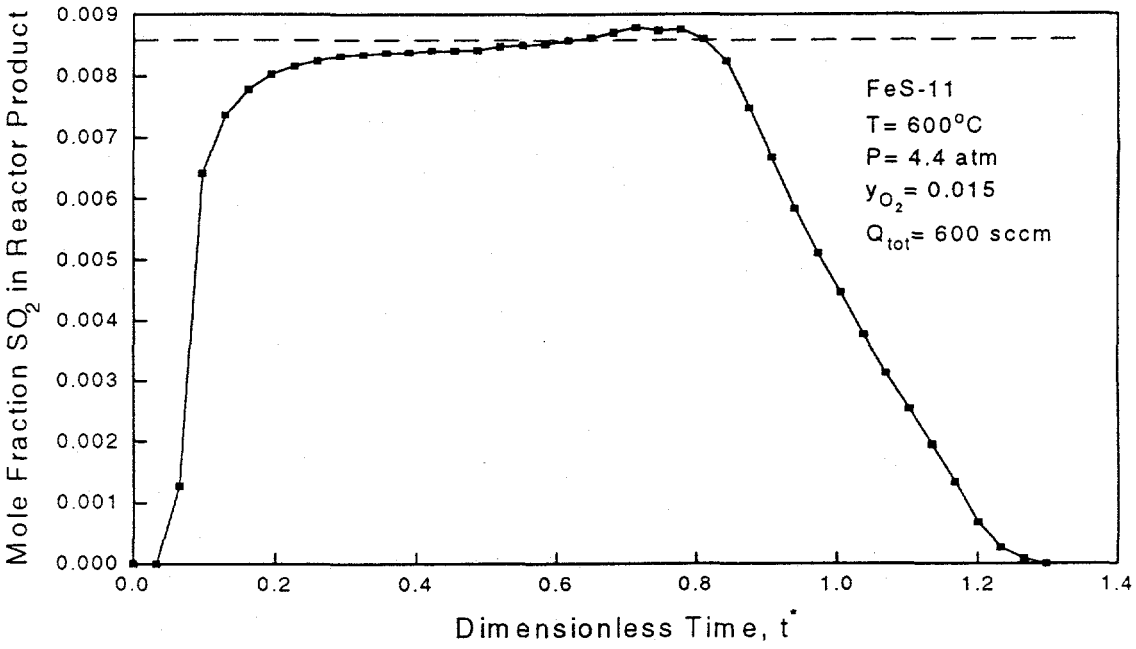

Figure 11. Fixed-Bed Reactor Response: H_2O regeneration, Run FeS-14

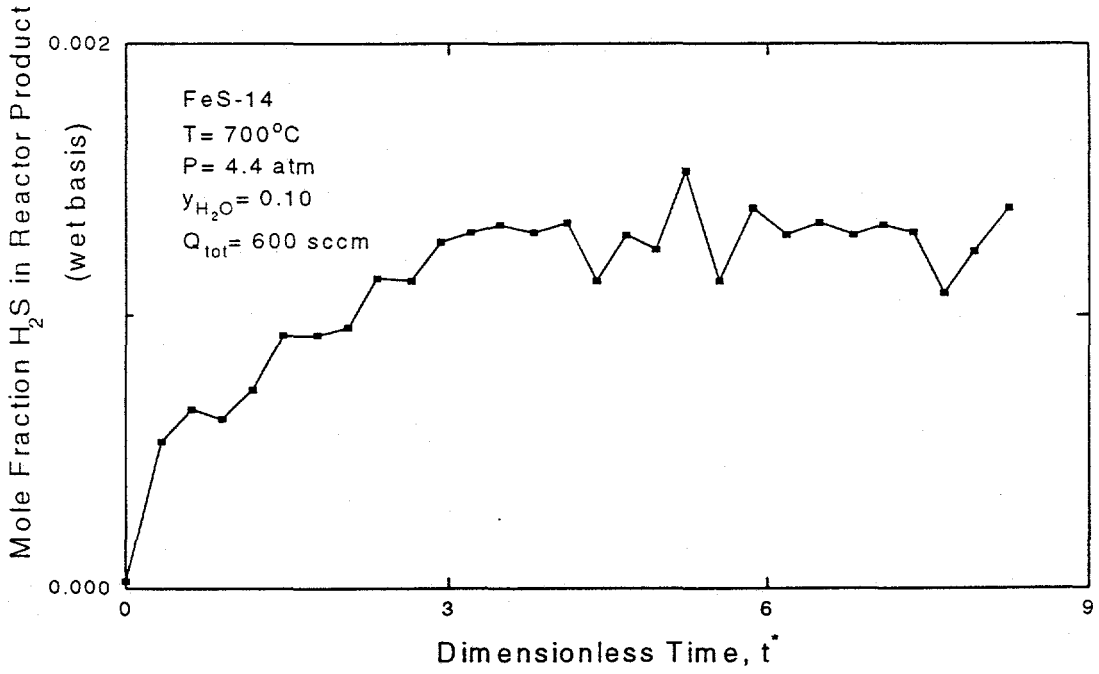

Figure 12. Fixed-Bed Reactor response: H_2O Regeneration, Run FeS-14

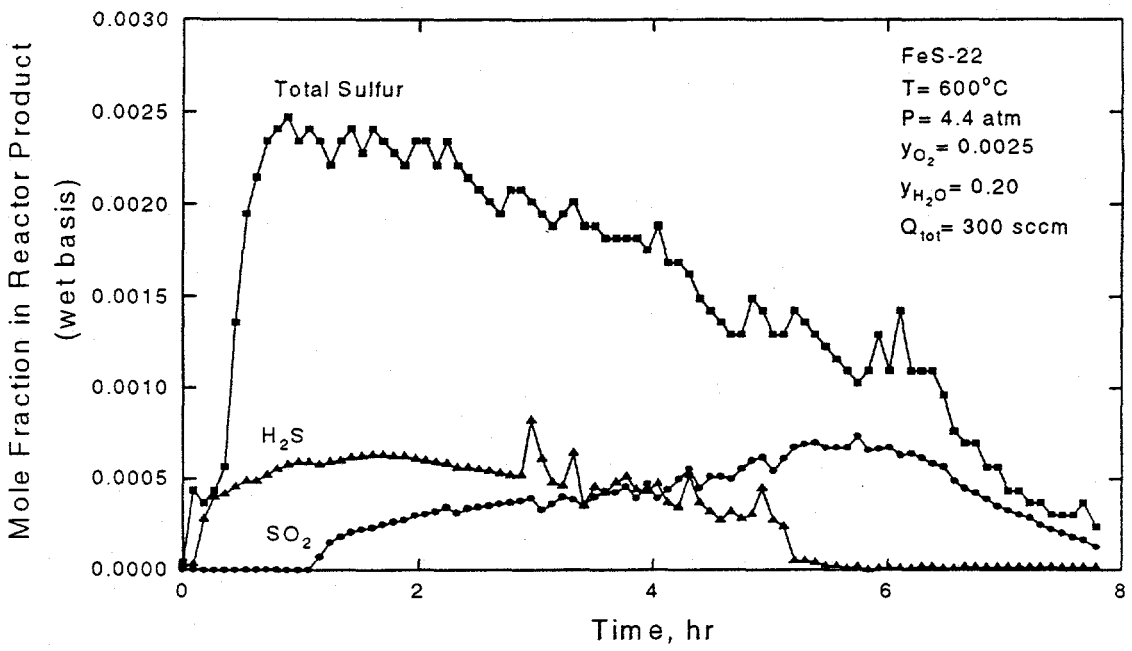

Figure 13. Fixed-Bed Response: H_2O and O_2 Regeneration, Run FeS-22

The cumulative production of each sulfur species as a function of time was determined by numerical integration of the concentration-time data. The cumulative amounts produced at the end of the reaction provided a check on the overall sulfur material balance. Results of the numerical integration of the run FeS-22 data are shown in Figure 14. The production of H_2S, H_2S+SO_2, and total sulfur, all expressed as a fraction of the theoretical sulfur associated with the initial FeS charge, are plotted versus reaction time. After the brief time delay, the amount of H_2S gradually increased to account for about 21% of the theoretical sulfur after 5.1 hours; no more H_2S was produced after that time. The H_2S and H_2S+SO_2 curves coincided for the first hour when no SO_2 was produced. Thereafter, the curves diverged and the cumulative production of H_2S+SO_2 was 45% of theoretical by the end of the run; this corresponds to cumulative SO_2 production of 24% of theoretical. The overall sulfur material balance for this run was quite good as the cumulative production of total sulfur by the end of the run was 99% of theoretical. Thus, about 55% of the sulfur was liberated in elemental form.

The instantaneous selectivity of elemental sulfur in run FeS-22 is shown in Figure 15. Selectivity is defined by

$$S(t) = \frac{Elemental\ Sulfur}{Total\ Sulfur} = \frac{Total\ Sulfur - (SO_2 + H_2S)}{Total\ Sulfur}$$

Although there is significant scatter in the results, particularly near the beginning and end of the run where $H_2S + SO_2$ concentration is approximately equal to total sulfur concentration, there is a clear trend to the data. Near the beginning, about 80% of the sulfur was released in elemental form. This was followed by a more or less linear decrease to near 20% at the end of the run. The cumulative, or time average, selectivity was, as shown in Figure 14, about 55%.

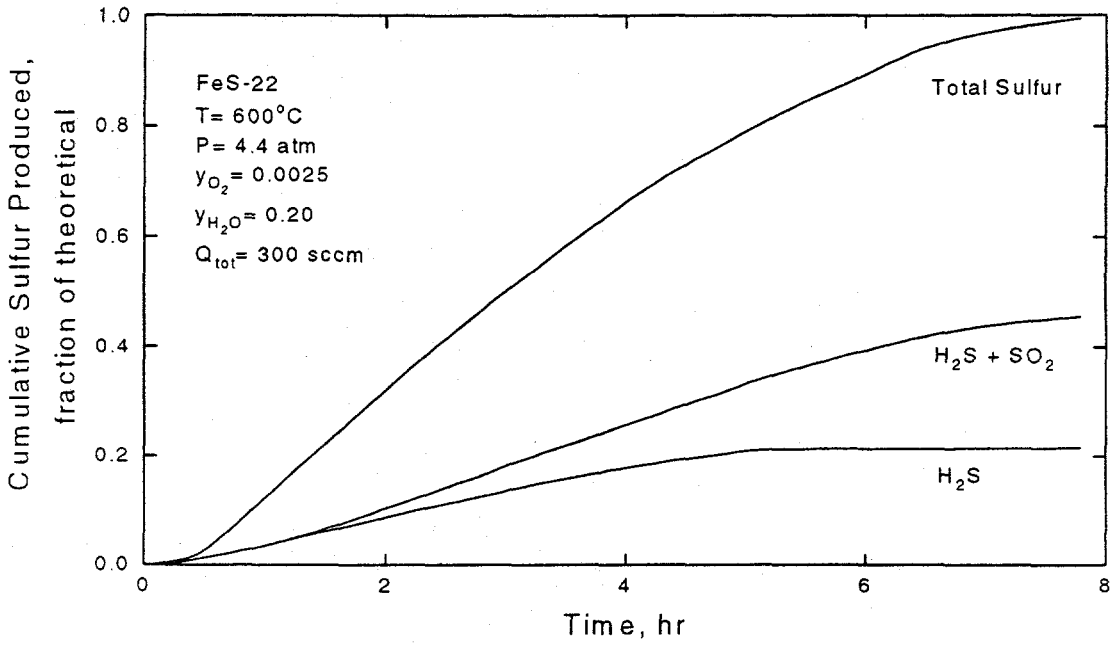

Figure 14. Cummulative Production of H_2S, H_2S+SO_2, and Total Sulfur, Run FeS-22

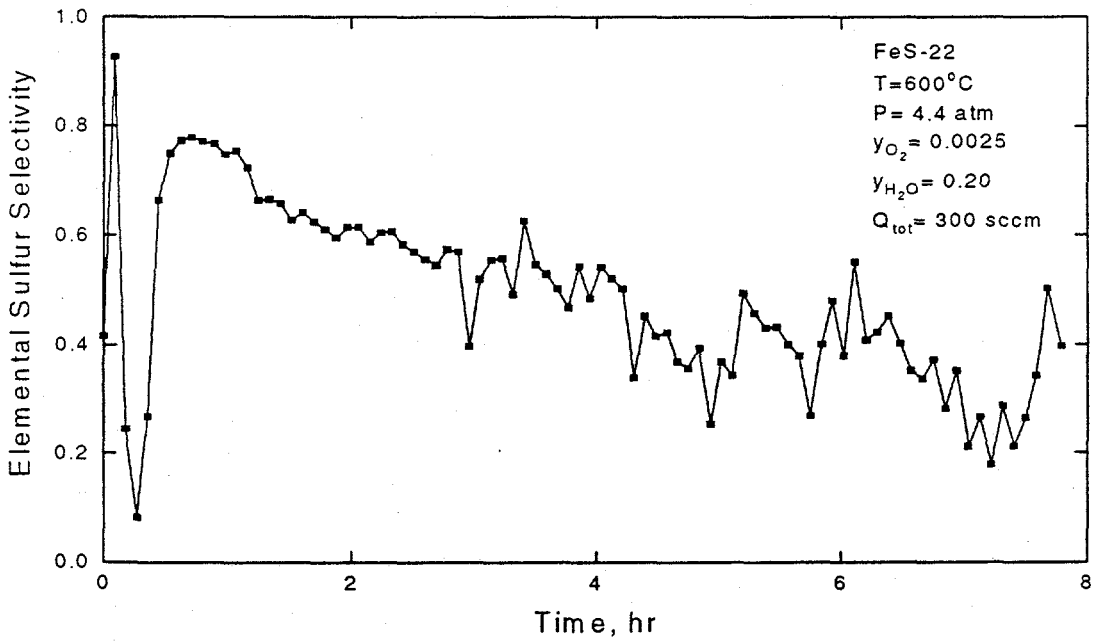

Figure 15. Instantaneous Selectivity to Elemental Sulfur, Run FeS-22

Maximum elemental sulfur selectivity occurred at low temperature, small regeneration gas flow rate, and large H_2O-to-O_2 ratio. The minimum temperature for complete regeneration was about 600°C. At lower temperatures, for example at 550°C used in run FeS-04, regeneration was incomplete, presumably because stable $Fe_2(SO_4)_3$ was formed. However, there was no indication of $Fe_2(SO_4)_3$ at 600°C or above, as shown by the results of run FeS-22.

Concentration-time results from run FeS-19 at the higher temperature of 700°C are shown in Figure 16. Reaction conditions other than temperature were identical in runs FeS-19 and FeS-22. The concentration-time responses were qualitatively similar as were the total run duration, maximum concentration of total sulfur, and the time corresponding to the total sulfur maximum. However, the maximum SO_2 concentration was about 50% larger at the higher temperature and the maximum occurred at an earlier time. The largest differences was associated with H_2S where maximum concentration doubled and the time corresponding to the maximum was reduced by about 25%. Numerical integration showed that only about 40% of the sulfur in run FeS-19 was released in elemental form.

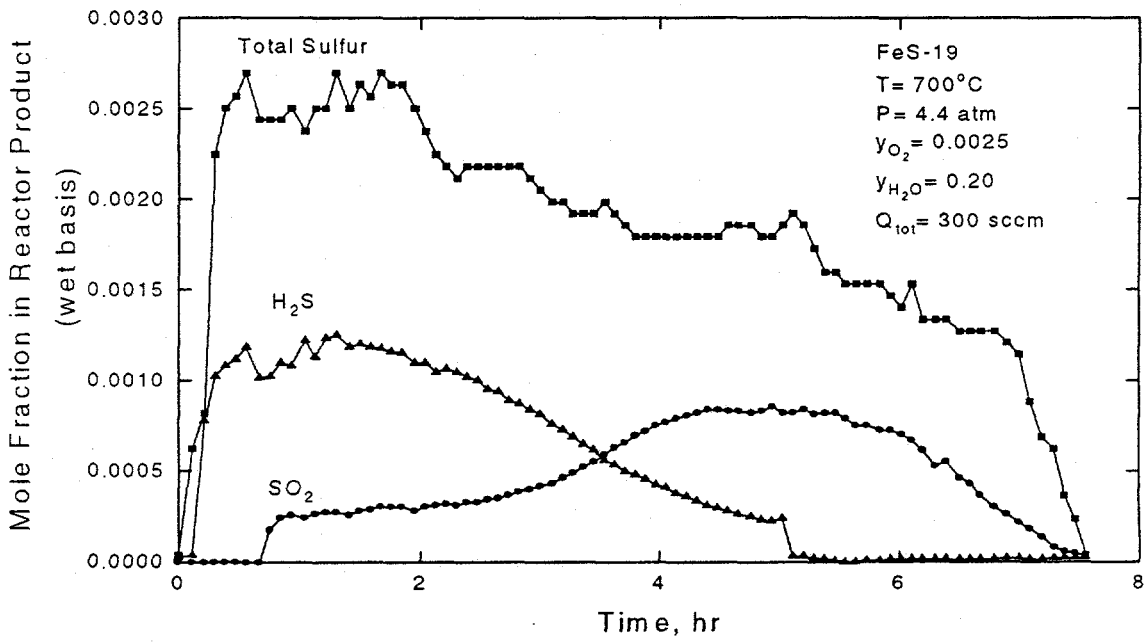

Figure 16. Fixed-Bed Reactor Response: H_2O and O_2 regeneration, Run FeS-19

Doubling the regeneration gas feed rate from 300 sccm in run FeS-22 to 600 sccm in FeS-26, while keeping other regeneration conditions constant, had a moderate negative effect on elemental sulfur production. The H_2S and SO_2 responses with time were similar to those shown in Figures 13 and 16, but the maxima were at larger mol fractions. Slightly less than 50% of the sulfur was liberated in elemental form in run FeS-26 compared to 55% in FeS-22. Varying the H_2O-to-O_2 ratio produced the largest effect on elemental sulfur selectivity. This may be seen by comparing the concentration-time results of run FeS-16 using a H_2O-O_2 ratio of 6.7 (Figure 17) and run FeS-25 using a H_2O-O_2 ratio of 200 (Figure 18) with the results from run FeS-22 at a H_2O-O_2 ratio of 80

(Figure 13). At small H_2O-O_2 ratio, as shown in Figure 17, the sum of the H_2S and SO_2 concentrations was approximately equal to the total sulfur concentration, indicating that the amount of elemental sulfur produced was quite small. Although the higher temperature and larger feed rate in run FeS-16 also contributed to reduced elemental sulfur formation, these effects were insufficient to explain the almost total absence of elemental sulfur.

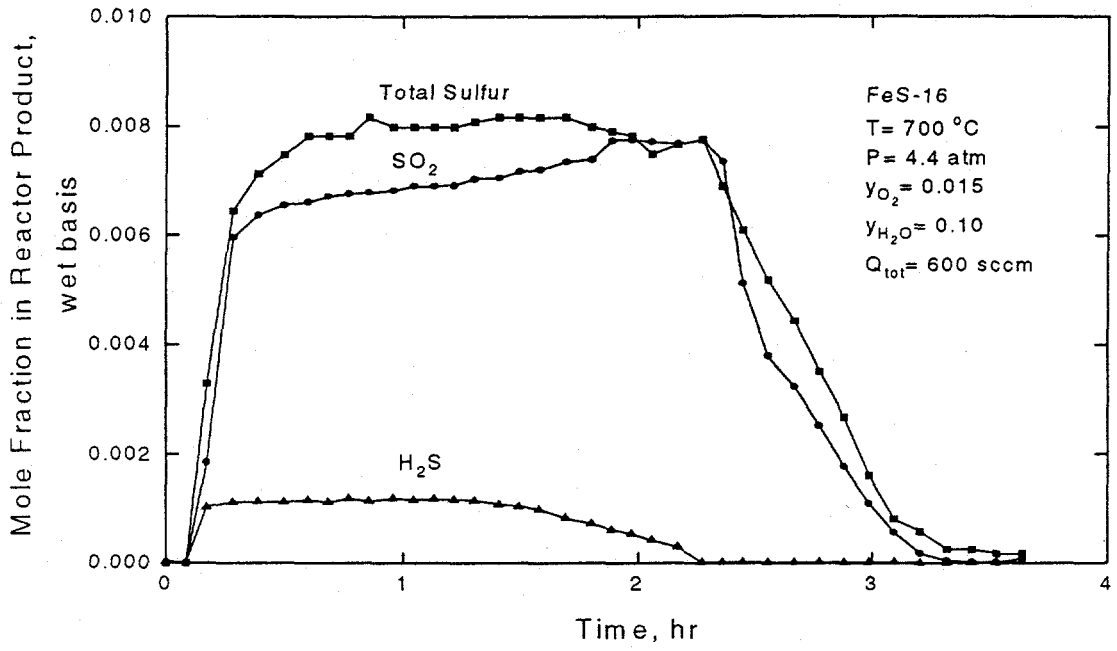

Figure 17. Fixed-bed Reactor response: H_2O and O_2 Regeneration, Run FeS-25

When the H_2O-O_2 ratio was increased to 200 in run FeS-25 (Figure 18), the cumulative elemental sulfur selectivity increased to 75%. Although the feed rate in FeS-25 was somewhat larger than in FeS-22, the larger feed rate should, based on previous discussion, reduce the elemental sulfur yield. With the exception of the large early peak in total sulfur concentration, the results in Figure 18 are qualitatively similar to other time-conversion results. The cumulative yields of H_2S and SO_2 in FeS-25 were only 15% and 10% of theoretical, respectively, and about 75% of the sulfur was liberated in elemental form.

Interpretation

The results of the FeS regeneration tests may be interpreted on the basis of reactions (6) through (9). Consider Figure 19a which shows proposed solid and gas concentration profiles within the sorbent bed during the early stages of the reaction, corresponding to just less than one hour in run FeS-22 (Figure 13). Because of the large rate of the FeS-O_2 reaction, the reaction interface separating Fe_2O_3 and FeS is quite steep. Only a small amount of Fe_3O_4, as indicated by the almost horizontal line extending from the FeS-Fe_2O_3 interface to the reactor exit, is present because the FeS-

H_2O reaction is slow. Fe_3O_4 will exist only downstream of the Fe_2O_3-FeS interface since Fe_3O will be quickly oxidized to Fe_2O_3 when contacted by O_2.

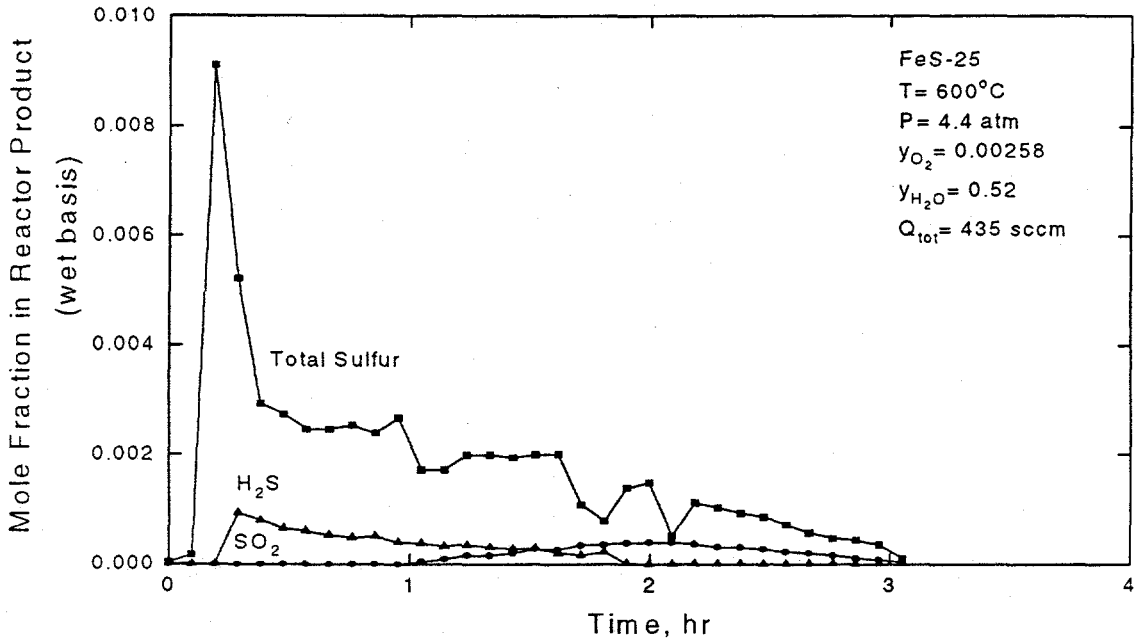

Figure 18. Fixed-Bed Reactor Response: H_2O and O_2 Regeneration, Run FeS-25

The shape of the O_2 concentration profile is approximately equivalent to the Fe_2O_3-FeS interface, but with minimal distortion due to the additional consumption of O_2 in converting Fe_3O to Fe_2O_3. Inlet H_2O concentration is much larger than inlet O_2 concentration (the H_2O-O_2 ratio in run FeS-22 is 80) and no H_2O reacts upstream of the Fe_2O_3-FeS interface. Downstream of the interface there is a small, almost linear, decrease in the H_2O concentration.

Proposed SO_2 and H_2S concentration profiles in the absence of the Claus reaction (reaction (8)) are shown by the solid lines in Figure 19a. The SO_2 concentration profile is quite steep and rises to a value equal to 57% of the inlet O_2 concentration as specified by reaction (6). The H_2S concentration is zero to the position of the Fe_2O_3-FeS interface and increases almost linearly from there to the bed exit. The final H_2S concentration is equal to 75% of the change in H_2O concentration according to reaction (7). At positions within the reactor where SO_2 and H_2S co-exist, elemental sulfur may be formed by the Claus reaction (8), and SO_2 and H_2S concentration profiles are modified as shown by the dotted lines in Figure 19a. No additional SO_2 may be formed downstream of the Fe_2O_3-FeS interface where the O_2 concentration is zero. Hence, the SO_2 concentration reaches a maximum at some interior bed position and decreases thereafter. In contrast, no H_2S is formed upstream of the Fe_2O_3-FeS interface, and additional H_2S is formed downstream of the point where the SO_2 concentration is zero.

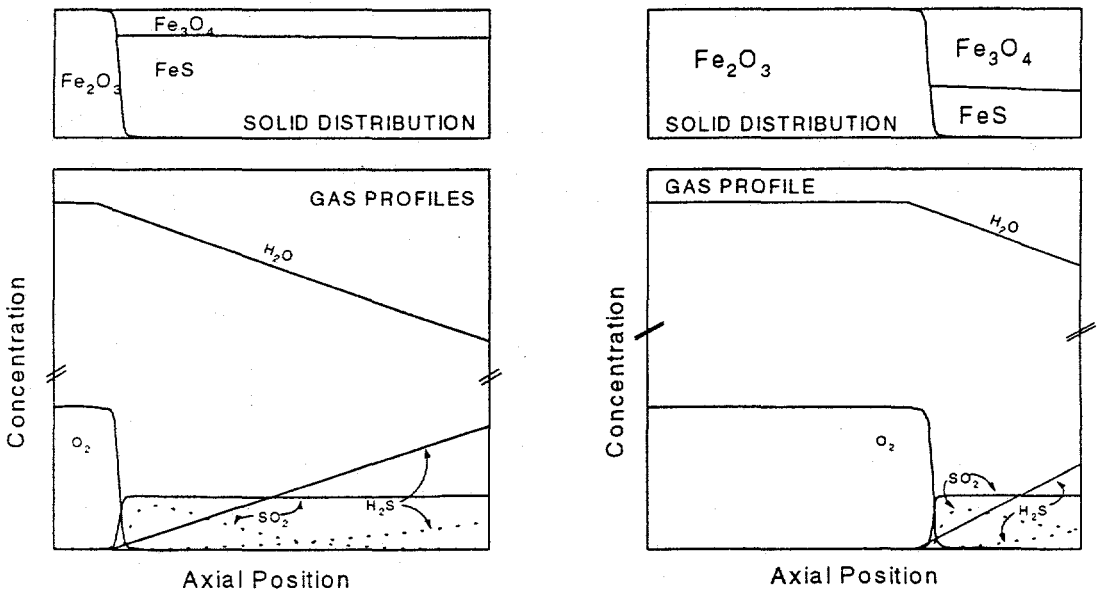

(a) at an Early Stage of the Reaction (b) at an Intermediate Stage of the Reaction

Figure 19. Proposed Solids Distribution and Gas Concentration Profiles within the Sorbent Bed

The quantity of SO_2 formed within the bed is almost independent of time prior to O_2 breakthrough. The only difference is the axial position at which the SO_2 is produced. In contrast, the quantity of H_2S formed is a maximum initially and decreases continuously with time as the Fe_2O_3-FeS interface moves through the bed. The maximum amount of H_2S coupled with the maximum contact time between SO_2 and H_2S is responsible for the elemental sulfur selectivity being maximum initially and decreasing with time. Because the fixed quantity of SO_2 contacts the maximum amount of H_2S for the maximum amount of time during the early stages of the reaction, all of the SO_2 reacts which leads to zero SO_2 product gas concentration. H_2S product concentration is not zero, however, since additional H_2S is formed downstream of the point where the SO_2 concentration is zero.

As the reaction progresses, the Fe_2O_3-FeS interface moves further into the bed and the concentration profiles are modified as shown in Figure 19b. These profiles correspond to a reaction time of about 4 hours in run FeS-22 (Fig. 13). The shape of the Fe_2O_3-FeS interface is similar to that at the earlier time, but displaced to the right. Again, no Fe_3O_4 exists to the left of the Fe_2O_3-FeS interface. To the right of the interface, the Fe_3O_4 profile remains almost horizontal but the concentration is increased due to the increased reaction time. The O_2 concentration profile is also similar to the earlier O_2 profile, but displaced to the right. The H_2O profile remains flat, but even less H_2O reacts because of the reduced contact time downstream of the Fe_2O_3-FeS interface. In the absence of the Claus reaction, the SO_2 concentration profile (solid line) is unchanged except for downstream position. The H_2S profile (solid line) is also similar, but initial H_2S formation is delayed because of the shift in the Fe_2O_3-FeS interface and the final H_2S concentration is smaller because of the reduced reaction time. When the Claus reaction is present (dashed lines), less SO_2 is consumed because less H_2S is present and the contact time is less. Therefore, both SO_2 and H_2S appear in the product gas.

The effects of flow rate, temperature, and H_2O/O_2 ratio on elemental sulfur production are consistent with the above interpretation. Doubling the feed gas rate from 300 to 600 sccm (runs FeS-22 and FeS-26) increased the selectivity to SO_2, had little effect on H Ş selectivity, and, as a consequence, reduced the elemental sulfur selectivity. The increased flow rate caused no change in the SO_2 production rate. However, less H_2S was formed due to the reduced residence time, and there was less time for the Claus reaction to occur. These effects tended to cancel to produce essentially no change in H_2S production, and left more SO_2 and less elemental sulfur in the product.

Higher temperature, in contrast, increased the H_2S yield, had little effect on the amount of SO_2 produced, and caused the elemental sulfur selectivity to decrease. This is consistent with the electrobalance results which showed that the FeS-H_2O reaction was more sensitive to temperature than the FeS-O_2 reaction (compare Figures 3 and 6). Although more H_2S was formed, much of it was formed downstream of the Fe_2O_3-FeS reaction front and had less opportunity to react with SO_2.

The strong effect of H_2O/O_2 ratio on elemental sulfur selectively, which ranged from almost zero at a ratio of 6.7 (Figure 17) to about 75% at a ratio of 200 (Figure 18), is also due to the large difference in the reaction rates of FeS with O_2 and H_2O. Large elemental sulfur selectivity requires that a large fraction of the FeS react with H_2O to liberate H_2S, and, of equal importance, that both H_2S and SO_2 be formed at positions within the bed which provides sufficient time for the Claus reaction to occur. H_2S formed near the exit of the bed is swept out of the reactor without having a chance to be converted to elemental sulfur.

Summary

While reasonably large selectivities to elemental sulfur are possible at large H_2O/O_2 ratios, the elemental sulfur concentration in the product gas was always quite small and the relatively low temperature required to condense the sulfur would result in the condensation of large quantities of steam. The large steam requirement and the large heat duty of the sulfur condenser, coupled with the difficulty of handling the sulfur and water mixture, are believed to make this concept impractical.

CERIUM OXIDE STUDIES

Regeneration of cerium oxysulfide, Ce_2O_2S, which is the product of the reaction between CeO_2 and H_2S was chosen for the second phase of the exploratory test series. Since Ce_2O_2S is not available commercially, it was necessary to carry out both the sulfidation and regeneration reactions. However, primary emphasis in the exploratory phase was given to the regeneration step. SO_2 served as the oxidizing agent in regeneration. The important reactions are

$$2CeO_2(s) + H_2S(g) + H_2(g) ==> Ce_2O_2S(s) + 2H_2O(g) \quad (10)$$

$$Ce_2O_2S(s) + SO_2(g) ==> 2CeO_2(s) + S_2(g) \quad (11)$$

Fixed-Bed Reactor

Only minor modifications to the fixed-bed reactor system shown in Figure 9 were required. The sulfidation gas consisted of H_2S, H_2, and N_2 while SO_2 and N_2 mixtures were used in the regeneration studies. Flow rates of these gases were controlled by mass flow controllers. The room temperature vapor pressures of H_2S and SO_2 limited the sulfidation and regeneration pressures to 5 atm and 1 atm, respectively.

Product gas exited from the bottom of the reactor, and, after flowing through a condenser, a sequence of filters, and a back pressure regulator, the composition was determined by gas chromatography. The exit line between the reactor and condenser was heat traced to minimize condensation of elemental sulfur during the regeneration tests.

The gas chromatograph was equipped with a thermal conductivity detector which measured H_2S concentration during sulfidation tests and SO_2 concentration during regeneration, both as a function of time. Since both the sulfidation and regeneration reactions were stoichiometrically "clean," it was not necessary to use the total sulfur analyzer, which greatly simplified the analysis compared to the FeS partial oxidation regeneration tests.

Initial sulfidation tests were plagued with "over-sulfidation," that is, the apparent amount of H_2S removed greatly exceeded the stoichiometric quantity associated with the conversion of CeO_2 to Ce_2O_2S. The formation of Ce_2S_3 instead of Ce_2O_2S was initially suspected as the cause of the over sulfidation. This explanation was later rejected when increasing the oxygen content of the feed gas (by the addition of CO_2 and/or H_2O) did not alter the result. Reaction between H_2S and the walls of the stainless steel insert was later determined to be the cause of "over-sulfidation." Although the insert had been Alonized to prevent reaction, it was either ineffective at the 800°C temperature used for most CeO_2 sulfidation tests or had deteriorated during the FeS regeneration studies to the point that protection was no longer provided.

The problem was ultimately solved by replacing the stainless steel insert with a quartz insert shown in Figure 20. While not totally eliminating contact between H_2S and high temperature steel surfaces, contact was minimized to the point that sulfur material balance closure in subsequent sulfidation tests has typically been within ±10% of stoichiometric. The quartz insert is attached to the top of the pressure vessel by a stainless steel ring and o-rings which fit over the shoulders at the top of the insert. These o-rings do not provide a pressure seal, but prevent gas by-passing and supply a flexible cushion to accommodate differences in the thermal expansion coefficients between the quartz and stainless steel. Dimples located near the bottom of the insert within the isothermal zone of the furnace support a porous quartz disk, a layer of quartz wool, and then the sorbent. The fragility of the quartz insert requires that extreme care be exercised when loading and unloading sorbent and assembling and disassembling the reactor. However, the arrangement has proven to be quite reliable and only one breakage has occurred during operation.

The primary operational problem has been caused by elemental sulfur plugging the tubing and filters between the reactor and chromatograph. As previously stated, the reactor product gas passes through a length of heated tubing into a condenser where most of the sulfur is removed and then through a sequence of filters before entering the chromatograph. The condenser contains quartz wool

to improve heat transfer characteristics and provide increased surface area to promote condensation. The current system has gradually evolved as successive problem sources were identified and corrected. Sulfur deposition outside of the condenser has not been eliminated but it has been reduced to a manageable level.

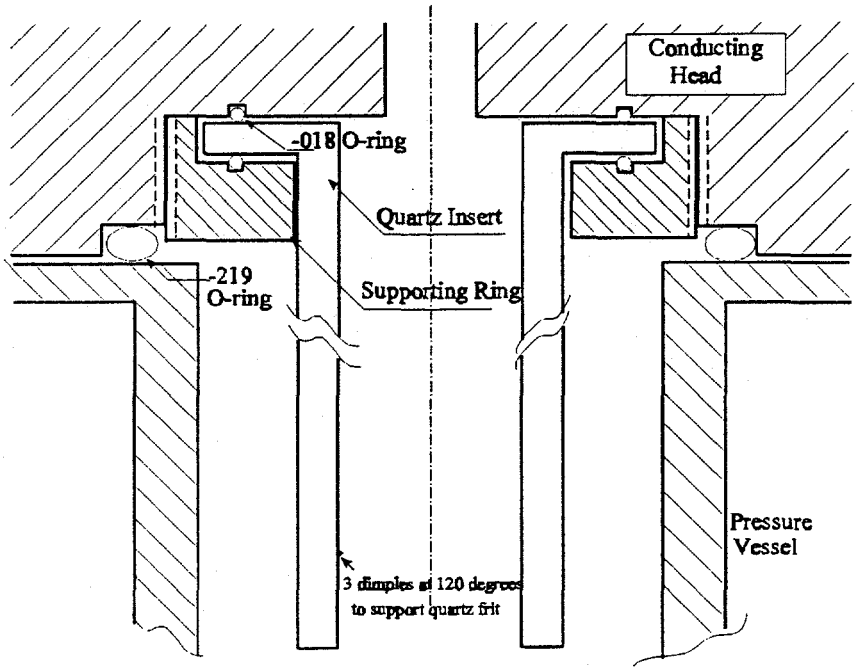

Figure 20. The Quartz Reactor Insert

Sorbent Properties

From 3 to 6 g of high purity CeO_2 from Rhone-Poulenc was used in all tests. Because of the extremely small particle size of the as-received material, pressure drop across the packed bed was approximately 3 atm which placed severe restraints on operating pressure in early tests. With any significant increase in pressure drop, the bed inlet pressure exceeded the SO_2 vapor pressure, thereby preventing SO_2 flow. This problem was solved by dry pressing the CeO_2 powder at 25,000 psi to form tablets, which were subsequently crushed and sieved. Particle size ranges between 150 and 300μ and between 75 and 150μ were used in later tests in which the bed pressure drop was only about 5 psi. Severe sintering was also encountered in early tests in which pure CeO_2 was used. At the conclusion of the test the sorbent was removed from the reactor as a single, highly porous cylinder. Shrinkage accompanied the sintering and provided an open path around the circumference of the reactor which allowed gas to bypass the sorbent. The sintering problem was solved by physically mixing CeO_2 with inert Al_2O_3 having a particle size range from 80 to 200μ to form the packed bed. The mixtures of Al_2O_3 and CeO_2 formed from the crushed tablets emerged from the reactor as free-flowing powders even after multicycle sulfidation-regeneration tests. Both 1-to-1 and 2-to-1 (by weight) mixtures of CeO_2-to-Al_2O_3 have been used without problems associated with sintering.

CeO_2 Sulfidation

Although the primary objective of the exploratory tests was to determine the feasibility of producing elemental sulfur directly during the regeneration of Ce_2O_2S using SO_2, it was necessary to begin by sulfiding CeO_2 since Ce_2O_2S could not be obtained commercially. Each regeneration test was preceded by sulfidation. The reaction parameters and range of reaction conditions studied is summarized in Table 3. The sulfidation gas composition was constant in all tests while pressure was always about 5 atm. In the early runs preceding the CeO_2 tableting step previously described, high bed pressure drop resulted in sulfidation pressures slightly above 5 atm. Temperature, gas flow rate, mass of CeO_2, and the CeO_2-to-Al_2O_3 ratio were varied in the preliminary test series.

Sulfidation results from an early "good" test are shown in Figure 21 in the form of a H_2S breakthrough curve. After 20 minutes, the H_2S concentration in the product gas increased to the 0.03% to 0.08% range and remained at that plateau level until 75 minutes. Active breakthrough then began, and an additional 25 minutes were required for the H_2S concentration to increase from 0.1% to 0.9%. A steady-state H_2S concentration of 0.99% was reached after 145 minutes elapsed time. Results of a non-reacting tracer test at the same conditions are also shown in Figure 21. The shaded area between the two curves is proportional to the quantity of H_2S removed by reaction with CeO_2. Numerical integration showed that the area corresponded to 102% of the stoichiometric sulfur associated with complete conversion of CeO_2 to Ce_2O_2S.

The CeO_2 tableting procedure was used for the first time in run Ce-09s01. The mass of CeO_2 was the same in both Ce-08s01 and Ce-09s01 but less Al_2O_3 was used in Ce-09s01 in order to maintain the total bed volume approximately constant. Other reaction conditions were the same in the two runs. The similarity of the H_2S breakthrough curves shown in Figures 21 and 22 in terms of the prebreakthrough plateau, the times corresponding to the beginning of breakthrough, and the slopes of the active portion of the breakthrough curves shows that the larger CeO_2 particle size and the different CeO_2-to-Al_2O_3 ratio had little effect other than to reduce bed pressure drop. All tests subsequent to Ce-09 used the larger CeO_2 particles obtained from the crushed tablets.

Table 3. Reaction Parameters in Preliminary CeO_2 Sulfidation Studies

Parameter	Range of Conditions
Temperature, °C	350 to 850
Pressure, atm	5.0 to 5.4
Gas Composition	1% H_2S
	10% H_2
	balance N_2
Gas Flow Rate, sccm	200 to 400
Mass of CeO_2, g	3.0 to 6.0
CeO_2 to Al_2O_3 Ratio	0.5 to 2.0

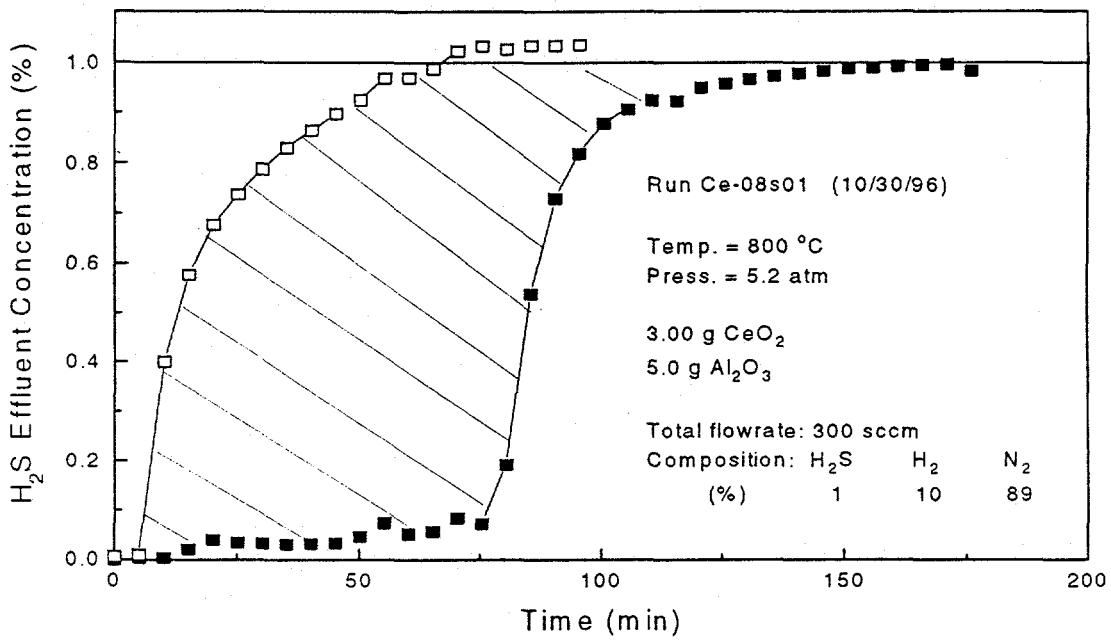

Figure 21. Fixed-Bed Reactor Response: H_2S Breakthrough, Run Ce-08s01

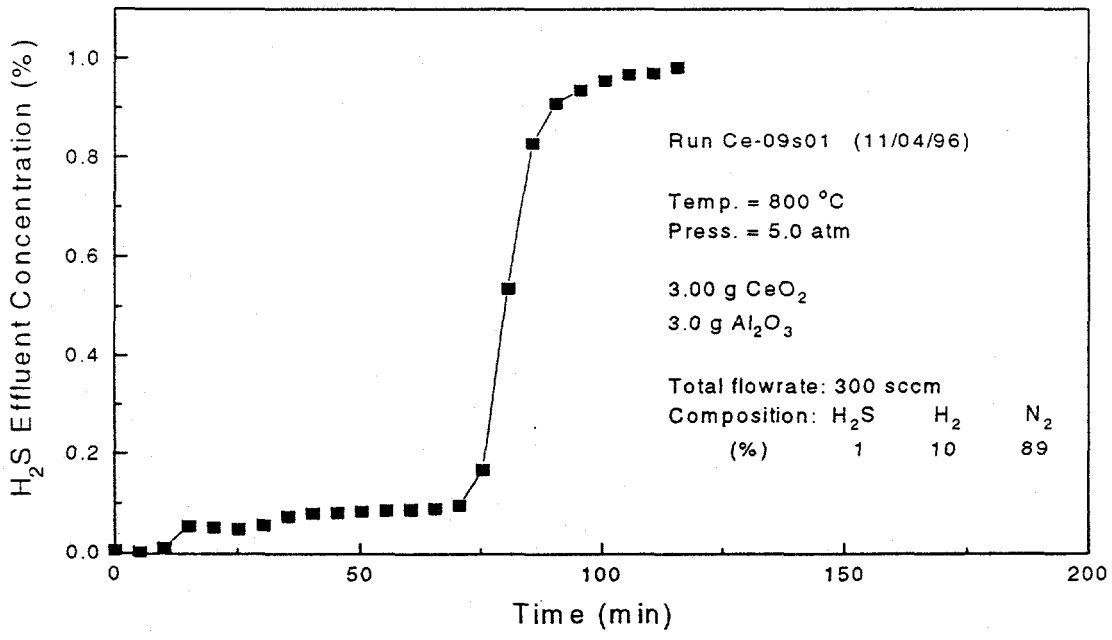

Figure 22. Fixed-Bed Reactor Response: H_2S Breakthrough, Run Ce-09s01

Most sulfidation tests were carried out at 800°C, and the effect of temperature over the range of 700°C to 850°C is quite small as shown in Figure 23. Active breakthrough began after about 60 minutes at the lower temperatures of 700 and 750°C, and after 70 minutes at 800 and 850°C. The slopes of the active portions of the breakthrough curves were approximately equal at 750, 800 and 850°C, but the slope at 700°C was considerably smaller, indicating a decrease in the global reaction rate at the lowest temperature. The postbreakthrough steady-state H_2S concentrations varied from a low of 0.83% at 850°C to a high of 1.08% at 750°C. All steady-state concentrations except the 0.83% at 850°C were within acceptable limits associated with mass flow controller and analytical system errors. The 850°C test was repeated with effectively identical results, so that the reduced postbreakthrough concentration appears to be real. One possible explanation is the increasing importance of the H_2S reaction with the stainless steel pressure vessel at the highest temperature. Substitution of the quartz insert for the stainless steel insert minimized, but did not eliminate, contact between hot steel surface and product gas.

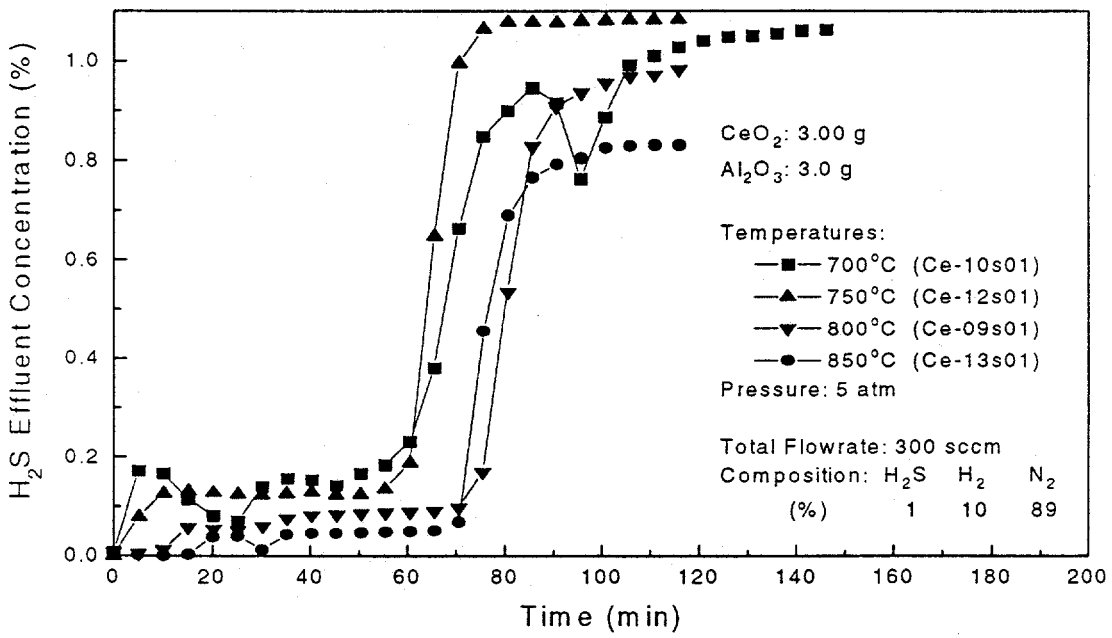

Figure 23. The Effect of Sulfidation Temperature

The prebreakthrough H_2S concentration plateau is also evident in each of the tests shown in Figure 23. The presence of the plateau was not initially a source of concern since primary interest was aimed at the production of elemental sulfur during regeneration. We now believe that the H_2S plateau is caused by reaction between H_2 in the sulfidation gas and elemental sulfur deposited in cooler sections of the reactor and downstream tubing during earlier regeneration tests. Evidence in support of this explanation is presented in Figure 24. Following a regeneration test, the reactor and downstream tubing were heated to 800°C and 350°C, respectively. 150 sccm of 10% H_2, balance N_2 was fed to the reactor, and quite large concentrations of H_2S were formed. An initial surge of about 0.5% H_2S was followed by a gradual decrease to a relatively constant level of 0.2%. After 160

minutes the temperature of the downstream tubing was reduced to 25°C and the gas flow rate was increased to 400 sccm. The H_2S concentration quickly decreased to about 0.01%.

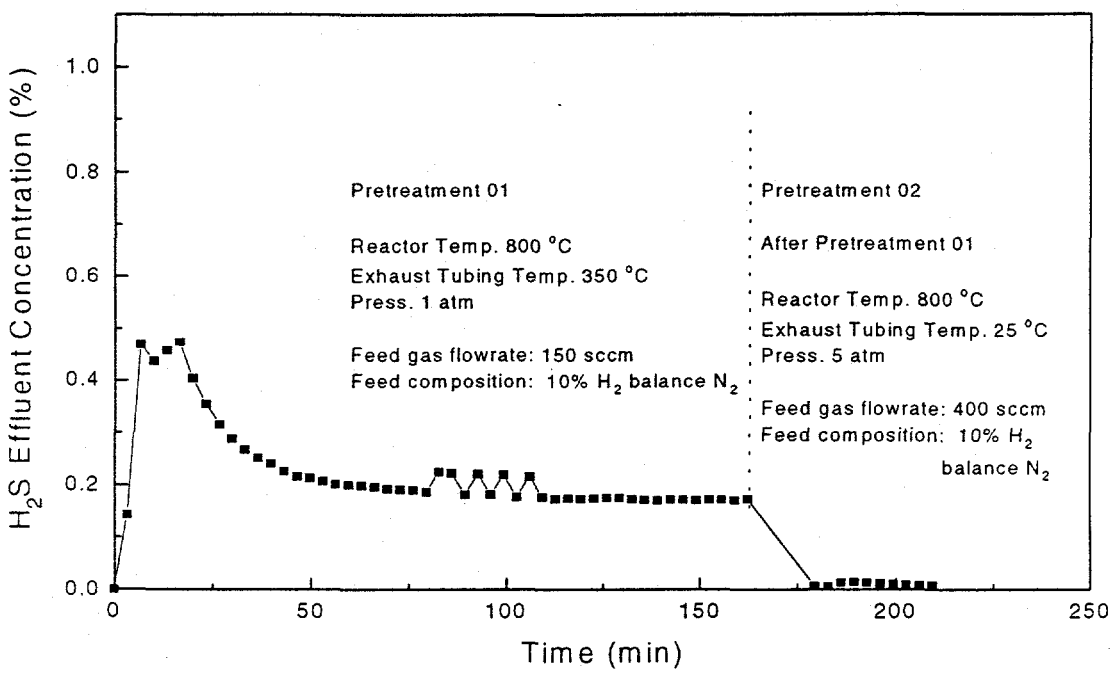

Figure 24. Reactor Cleaning Test: H_2S Formed by the Reaction of H_2 and Elemental Sulfur

The H_2S breakthrough curve from run Ce-16s03, the first sulfidation test following the cleaning procedure, is shown in Figure 25. The reduction in H_2S concentration during early portions of the run is obvious. The 0.01% H_2S during the first 20 minutes corresponds to 99% H_2S removal, and the removal remained above 95% for the first 80 minutes of the test. Other characteristics of the breakthrough curve, including the time corresponding to the beginning of active breakthrough and the slope of the active portion of the breakthrough curve, are similar to results from other sulfidation tests at the same conditions.

Additional cleaning studies (not shown) were conducted in which the reactor at 800°C and downstream tubing at 350°C were exposed to flowing air. Appreciable SO_2 was found in the product gas meaning that the H_2 cleaning was successful in removing most, but not all, of the sulfur contamination. This aspect has not been fully pursued since H_2S is analyzed using the thermal conductivity detector (TCD) whose H_2S sensitivity limit is about 100 ppmv (0.01%). Thus, the measured H_2S concentrations during the first 20 minutes of run Ce-16s03 are near the detection limit. More complete cleaning to further reduce the early H_2S concentration is of limited value until the analytical capability for H_2S is upgraded.

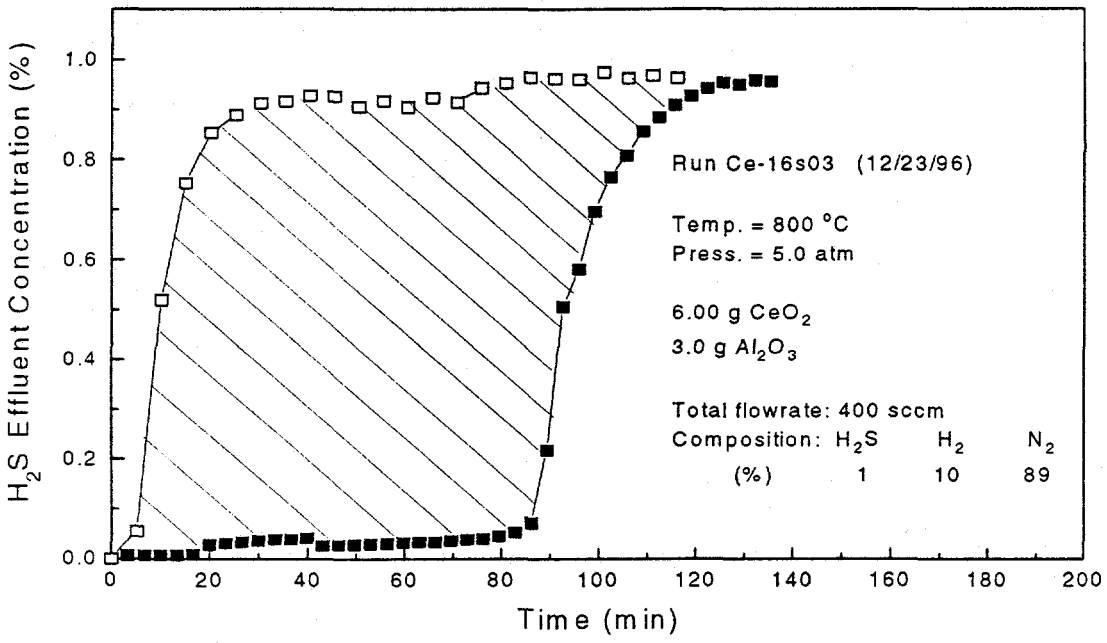

Figure 25. Fixed-Bed Reactor Response: H_2S Breakthrough Curve, Run Ce-16s03

Ce_2O_2S Regeneration

All regeneration tests were preceded by sulfidation. In addition, all regeneration tests described in the following paragraphs were carried out after the CeO_2 tableting procedure was adopted. For the cerium sorbent process to be economical, it is necessary that the elemental sulfur concentration in the regeneration product gas be reasonably large in order that the heat duty of the sulfur condenser and the quantity of recycle SO_2 be maintained at reasonable levels.

Reaction parameters and the range of regeneration conditions studied are summarized in Table 4. In the first regeneration test, the initial temperature tested was 350°C, and no reaction was observed. The temperature was then increased gradually and the reaction was found to be rapid at 600°C. All subsequent tests were conducted at 600°C. Most regeneration tests were conducted at 1.0 atmosphere to maximize the difference between the vapor pressure of SO_2 and the reactor operating pressure. Regeneration testing began using 1% SO_2 in N_2 and the SO_2 content in later tests was gradually increased to a maximum of 12% as we became comfortable with the behavior of the system. Early regeneration tests used a total flow rate of 300 sccm. However, as the SO_2 content increased, the duration of the run and the amount of data collected during the run decreased. Consequently, when the SO_2 content was increased to 12%, the flow rate was reduced to 200 sccm which, when coupled with changes in the chromatograph sampling frequency, provided sufficient data to establish the characteristics of the SO_2 breakthrough curve.

Table 4. Reaction Parameters in Preliminary Ce_2O_2S Regeneration Tests

Parameter	Range of Conditions
Temperature, °C	350 to 600
Pressure, atm	1.0 to 2.7
Gas Composition	1 to 12%
	balance N_2
Gas Flow Rate, sccm	200 to 300
Mass of CeO_2, g	3.0 to 6.0
CeO_2 to Al_2O_3 Ratio	1 to 2

The SO_2 breakthrough curve from an early regeneration test at 2.5 atm using 1% SO_2 is shown in Figure 26 along with the results of a non-reacting tracer test at the same conditions. The SO_2 concentration was effectively zero for the first 45 minutes while active breakthrough occurred in the 45 to 90 minute time span. A temporary upset in the 70 to 90 minute time period was responsible for the unusual shape of the breakthrough curve during that time. After about 100 minutes, the SO_2 concentrations from both the reaction and tracer tests reached steady-state values of 1.04%. According to reaction (11), the elemental sulfur concentration (considered as S_2) in the regeneration product is equal to the difference between the SO_2 concentrations of the feed and product gases. Thus, the elemental sulfur concentration in the product approached 1% for the major portion of the run. The area between the SO_2 breakthrough and tracer curves is proportional to the quantity of elemental sulfur liberated during the reaction. Numerical integration of this area corresponded to 104% of the stoichiometric amount of sulfur based on the initial solid being pure Ce_2O_2S. This value is in good agreement with the sulfur material balance during the preceding sulfidation cycle (Ce-09s01) which corresponded to sulfur removal of 110% of stoichiometric based on the initial solid being pure CeO_2. The sulfur material balance closures in both the sulfidation and regeneration phases of this test are typical. In most of the exploratory runs the sulfur material balance closure was within ±10% of stoichiometric.

SO_2 breakthrough curves for a number of regeneration tests using increasing SO_2 concentrations are shown in Figure 27. The concentration axis is normalized, i.e., the ratio of the product and feed concentrations, so that the results from all tests should approach a value of 1.0, which is indeed the case. The beginning of active breakthrough decreased from about 60 minutes to 30 minutes to 15 minutes to between 5 and 10 minutes as the SO_2 content increased from 1% to 2% to 4% and finally to 8%. Note that the 2%, 4%, and 8% tests were all part of run Ce-15, and represent the results of three separate sulfidation and regeneration cycles. Multicycle test results are covered in the following section. Also the four tests represent a range of regeneration pressures from 1 to 2.5 atm.

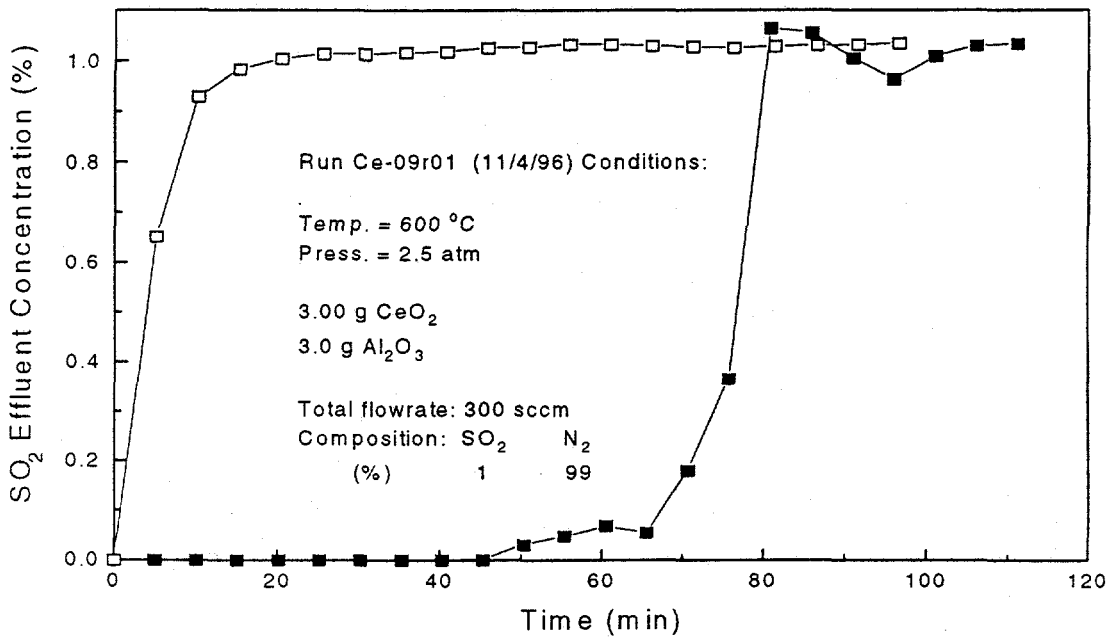

Figure 26. Fixed-Bed Reactor Response: SO_2 Breakthrough Curve, Run Ce-09r01

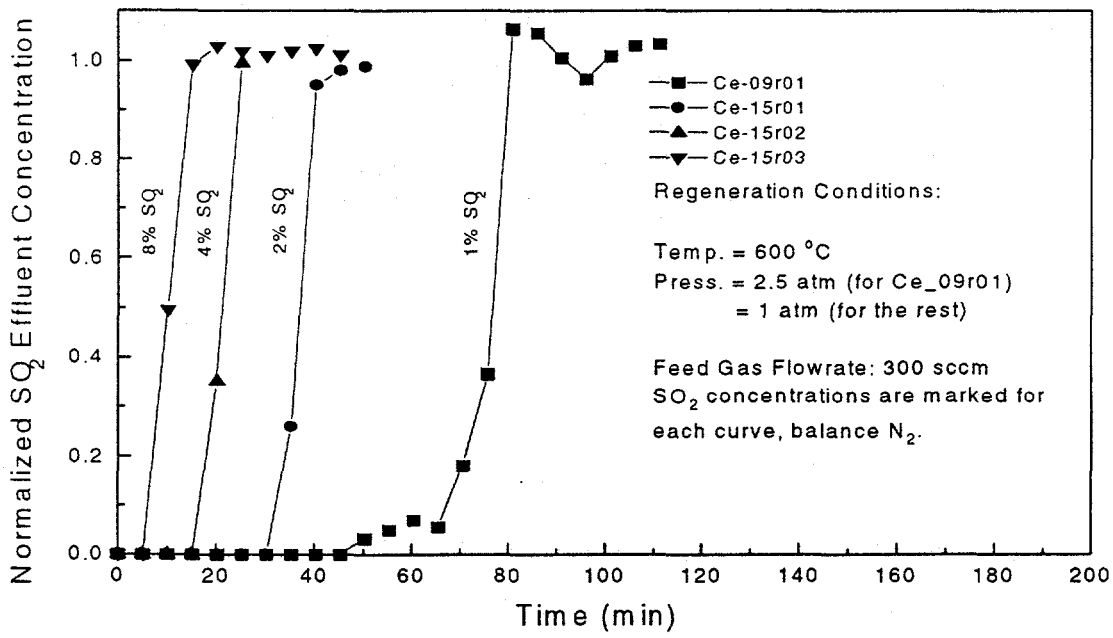

Figure 27. SO_2 Breakthrough Curves as a Function of SO_2 Content of the Feed Gas

With the exception of the SO_2 plateau in the 45 to 60 minute period of the test using 1% SO_2, the appearance of all of the breakthrough curves is similar. In particular, the slopes of the breakthrough curves using 2%, 4%, and 8% SO_2 are similar. However, as the concentration increased the duration of the tests decreased and fewer product gas samples were available to characterize the breakthrough curve. For example, regeneration using 8% SO_2 was effectively complete by the fourth sample about 16 minutes after the start of the test. The relative sparcity of the data may be responsible for the lack of the SO_2 concentration plateau at the higher SO_2 concentrations.

Because of the shorter duration and limited number of product gas concentration data points, it was obvious that changes in the operating conditions were required before further increases in SO_2 concentration could be made. The conclusion of the exploratory test phase called for a ten cycle run at still larger SO_2 concentration to provide preliminary information on the durability of the CeO_2 sorbent. Three significant changes were made prior to the multicycle test. The chromatograph operating conditions were altered to reduce the product gas sampling interval from 5.0 to 3.3 minutes. The regeneration gas flow rate was reduced from 300 to 200 sccm in order to maintain a constant SO_2 flow rate of 24 sccm while increasing the SO_2 content from 8% to 12%. Finally, the amount of the CeO_2 charge was doubled from 3.0 to 6.0 g. The amount of Al_2O_3 was constant at 3.0 g in each test.

Multicycle Test Results

The key to any high temperature desulfurization process is sorbent durability. Therefore a ten-cycle run, Ce-16, was conducted to provide preliminary information on the durability of the CeO_2 sorbent. Planned reaction conditions for the sulfidation and regeneration cycles are presented in Table 5. Unfortunately, an error in the total gas flow rate was made in the first sulfidation cycle, Ce-16s01, and results from this test are not included in the following discussion.

Table 5. Sulfidation and Regeneration Conditions for Ten-Cycle Test Ce-16

Reactor Charge

6.0g CeO_2
3.0g Al_2O_3

Sulfidation		Regeneration	
Temperature, °C	800	Temperature, °C	600
Pressure, atm	5	Pressure, atm	1
Gas Composition, %		Gas Composition, %	
H_2S	1	SO_2	12
H_2	10	N_2	88
N_2	89		
Flow Rate, sccm	400	Flow Rate, sccm	200

H_2S breakthrough curves for nine cycles, Ce-16s02 through Ce-16s10, are shown in Figures 28 and 29. Figure 28 is the traditional figure showing the entire breakthrough curve while in Figure 29 the concentration scale has been expanded to emphasize H_2S concentrations during the prebreakthrough period. Note that the breakthrough curve for Ce-16s08 is different from the other curves. The H_2S mass flow controller malfunctioned after 175 minutes causing the H_2S flow rate to decrease and producing the decreasing H_2S concentrations; this malfunction may have begun earlier and been responsible for the earlier differences in the Ce-16s08 breakthrough behavior as well.

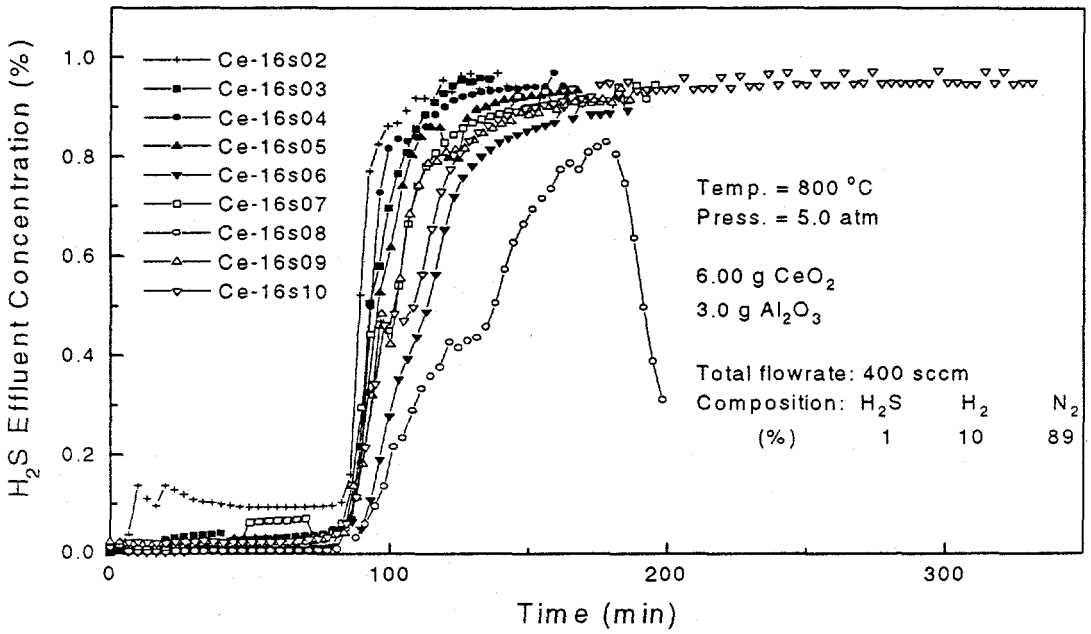

Figure 28. Fixed-Bed Reactor Response: H_2S Breakthrough Curves for Nine Sulfidation Cycles of Run Ce-16 Showing the Entire Breakthrough Curves

These figures show a wide variation in prebreakthrough behavior. The prebreakthrough concentration in Ce-16s02 is about 0.1% H_2S which corresponds to only 90% H_2S removal. However, in all other cycles the initial concentrations were equal to or less than 0.025% H_2S (250 ppmv), and, with the exception of the unexplained upset in Ce-16s07 during the 50 to 70 minute period, the H_2S concentrations were less than 0.05% (500 ppmv, 95% removal) for about 80 minutes in each cycle. Of particular interest, the concentrations in Ce-16s06 and Ce-16s08 were below 150 ppmv for the first 80 minutes. H_2S breakthrough time, which is taken to correspond to 0.05% H_2S, was approximately constant as shown in Figure 30. The breakthrough times ranged from 79.5 minutes in Ce-16s04 to 84.3 minutes in Ce-16s05 with no visible decrease as the cycle number increased. Results from Ce-16s01 and Ce-16s02 are omitted from the figure and the upset in Ce-16s07 was ignored in determining the breakthrough time.

The importance of sulfur contamination from preceding regeneration runs was discovered between cycles Ce-16s02 and Ce-16s03. Various cleaning procedures were used beginning with Ce-16s03 and all subsequent prebreakthrough concentrations were significantly lower. Most of the sulfur

contaminant was removed by flowing sulfur-free reducing gas through the reactor at 850°C and tubing located between the reactor and condenser heated to 350°C. The prebreakthrough concentrations in Ce-16s03 through Ce-16s10 in Figure 29 followed cleaning in the reducing gas. Reduction, however, was not sufficient to remove all sulfur compounds since significant SO_2 concentrations were formed when air flowed through the reactor and tubing at high temperature.

All ten regeneration cycles used the reaction conditions shown in Table 5, and SO_2 breakthrough curves for all cycles are shown in Figure 31. With the exception of two individual samples -- the first at 17 minutes in Ce-16r03 and the second at 10 minutes in Ce-16r10 -- the results

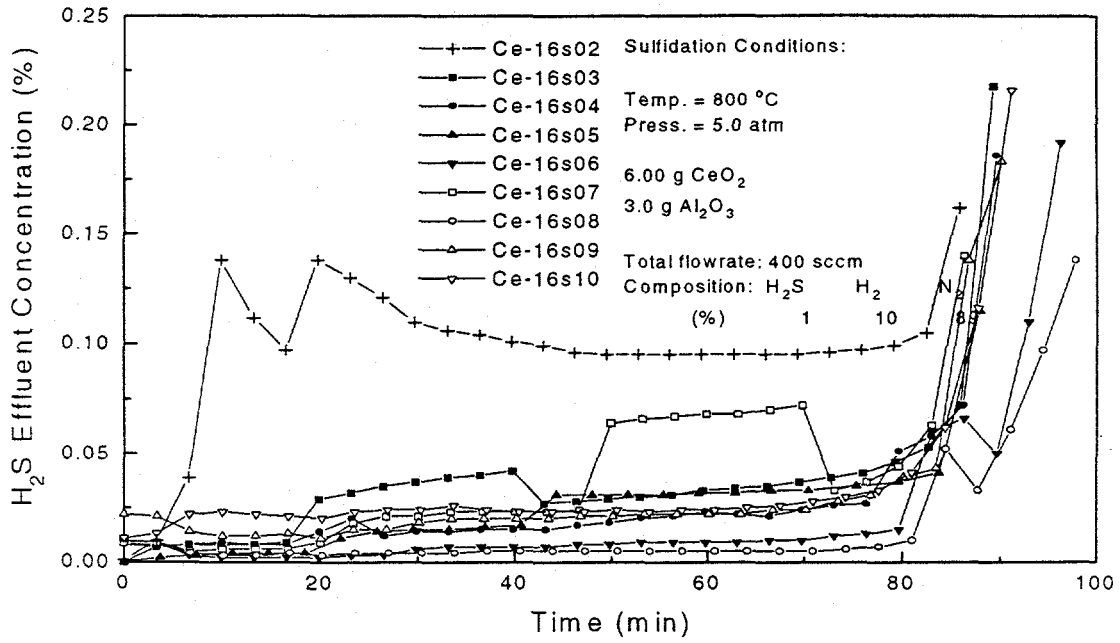

Figure 29. Fixed-Bed Reactor Response: H_2S Concentration During the Prebreakthrough Periods of Run Ce-16

were effectively identical. The first measurable concentration of SO_2, about 1%, was detected after 10 minutes, and by 23 minutes regeneration was effectively complete. The steady-state SO_2 content of the product gas ranged from 11.8% to 12.2%.

Sulfur material balance results, expressed as percent of stoichiometric sulfur removed during sulfidation and liberated during regeneration, are presented in Figure 32. Sulfur removed during sulfidation ranged from a minimum of 75.0% in Ce-16s02 to a maximum of 96.8% in Ce-16s10. No sulfidation results are presented for Ce-16s01 because of the flow rate error and for Ce-16s08 because of the H_2S mass flow controller malfunction. The low value in Ce-16s02 may be associated with the high prebreakthrough H_2S concentration (see Figures 28 and 29) caused by residual sulfur from the previous regeneration cycle. For the eight sulfidation cycles, H_2S removal averaged 87.2% of stoichiometric (88.9% of stoichiometric if the low value associated with Ce-16s02 is not considered).

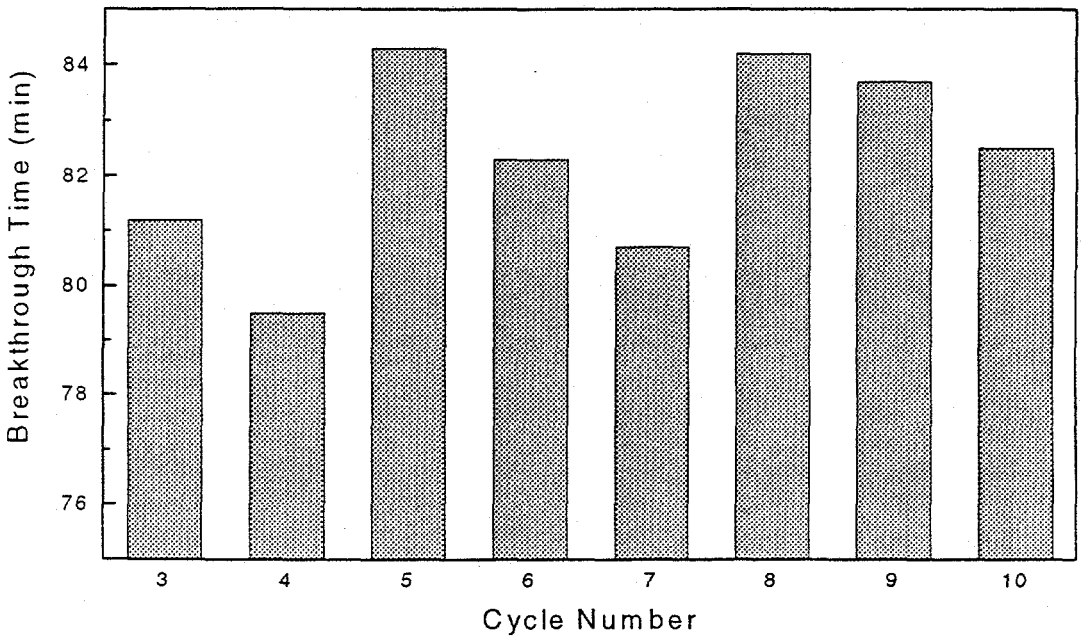

Figure 30. Breakthrough Times Corresponding to 0.05% H_2S in the Product Gas of Run Ce-16

Sulfur material balance during regeneration ranged from 86.1% stoichiometric in Ce-16r03 to 96.2% in Ce-16r10 with a ten-cycle average of 91.8% of stoichiometric. Ideally, the sulfidation and regeneration results from a single cycle should be identical. That is, the quantity of sulfur removed during sulfidation should be equal to the quantity liberated during regeneration. Differences are caused by errors in flow rates (mass flow controllers), product gas analysis and numerical integration of the breakthrough data. The maximum difference occurred in cycle 02 where sulfur removal was 75.0% of stoichiometric and sulfur liberation was 90.4% of stoichiometric. However, the agreement is quite good based on the average results of the entire test; as previously stated, the average sulfur removal from the eight sulfidation tests was 87.2% of stoichiometric (88.9% ignoring cycle 02) while the ten-cycle regeneration average was 91.8% of stoichiometric.

The overall results from this first extended test are considered to be quite favorable. The constancy of the slopes of the sulfidation and regeneration curves during active breakthrough, the small variation in breakthrough times, and the reasonable agreement in sulfur material balance during sulfidation and regeneration all suggest that little, if any, sorbent deterioration occurred.

Test Ce-16 ended the exploratory phase of the experimental program. Favorable experimental results coupled with reasonable economic projections from the process analysis effort (not discussed in this report) lead to the selection of the CeO_2 system for more detailed experimental testing. A brief description of plans for the remaining portion of the study is included in the following section.

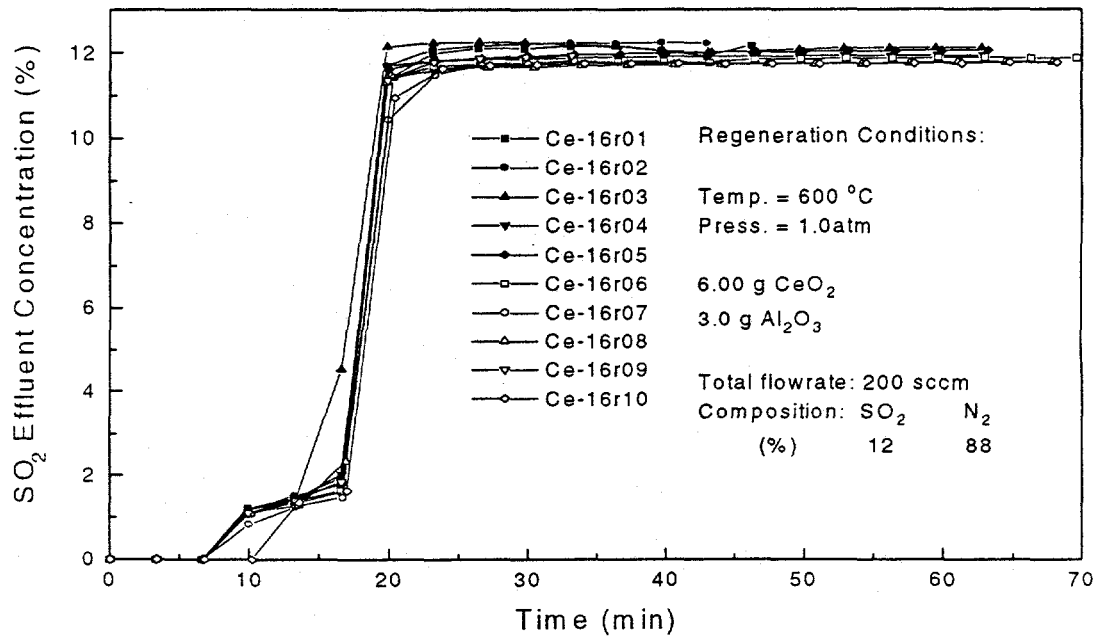

Figure 31. Fixed-Bed Reactor Response: SO_2 Breakthrough Curves for the Ten Regeneration Cycles of Run Ce-16

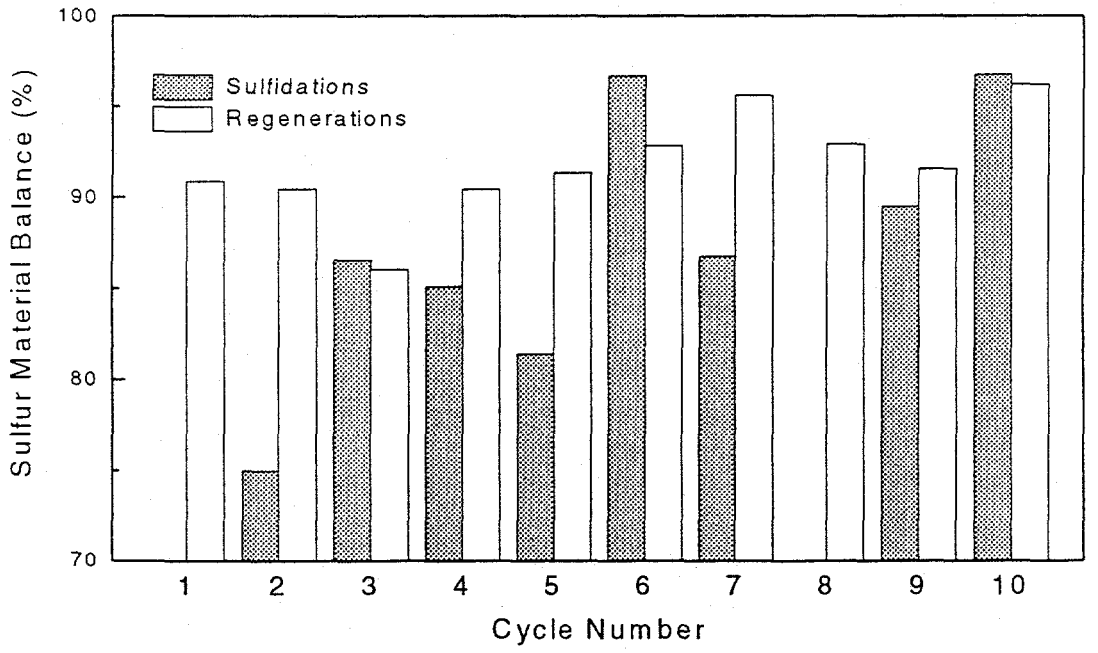

Figure 32. Sulfur Material Balance Closure During the Ten Sulfidation and Regeneration Cycles of Run-16

SUMMARY AND FUTURE EXPERIMENTAL WORK

The exploratory experimental phase of this project examined the regeneration of FeS under "partial oxidation" conditions and the sulfidation of CeO_2 with H_2S and regeneration of Ce_2O_2S with SO_2. The objective of both regeneration studies was the direct production of elemental sulfur

While large fractions of the sulfur in FeS can be successfully liberated in elemental form, the reaction must operate under O_2-starved conditions and with a large excess of steam. As a result, the elemental sulfur concentration of the regeneration product gas is judged to be too low for commercial application. Energy costs associated with providing the large amounts of steam, and subsequent cooling costs to recover elemental sulfur would be excessive.

In contrast, the regeneration of Ce_2O_2S with SO_2 proceeds rapidly at 600°C with stoichiometric production of elemental sulfur. As much as 12% elemental sulfur has been produced in the regeneration product gas during this exploratory effort, and there appears to be no fundamental reason why significantly higher concentrations cannot be produced. Essentially pure elemental sulfur can be separated by condensation with excess SO_2 recycled to the regeneration reactor. No evidence of CeO_2 sorbent deterioration was seen in a ten-cycle test. While numerous experimental problems caused by elemental sulfur condensing and plugging the laboratory-scale experimental apparatus were experienced, such problems should be relatively easy to control in a commercial process.

The potential problems with a CeO_2 process are concentrated in the desulfurization phase. The thermodynamics of the CeO_2-H_2S reaction are not sufficient under most circumstance to reduce the H_2S concentration to levels needed for IGCC operation. For this reason, a two-stage desulfurization process using CeO_2 for bulk H_2S removal followed by a polishing step using zinc sorbent has been proposed. Elemental sulfur would be produced during the regeneration of Ce_2O_2S while SO_2 formed during ZnS regeneration would be recycled to the gasifier and ultimately captured as elemental sulfur.

The required temperature for sulfidation of CeO_2 is approximately 800°C, considerably above the maximum temperature at which zinc sorbents are applicable. Although reduction of CeO_2 to CeO_n ($n<2$) is known to occur in highly reducing gases at sufficiently high temperature, no volatile products are formed as with Zn(g). Indeed, reduction and subsequent sulfidation of CeO_n offers promise for increased H_2S removal compared to CeO_2 and creates the possibility that a single-stage cerium sorbent process might by used in limited conditions. Determining the ultimate desulfurization capability of CeO_n provides a major objective for the remainder of the project.

The gas chromatograph currently used for gas analysis is equipped with a thermal conductivity detector whose sensitivity limit for H_2S is about 100 ppmv. A flame photometric detector will be acquired to enable the H_2S analysis to be extended to low (<10) ppmv levels. Sulfidation product gas analysis at these low H_2S concentrations will also require that the reactor and downstream tubing be free from sulfur contamination from previous regeneration tests. Modifications in the reactor system to insure the required level of cleanliness are being planned.

During the remainder of the study, the effects of reaction parameters such as temperature, pressure, gas flow rate and composition will be examined. CeO_2 from three sources will be tested and durability studies will be extended to at least 20 sulfidation-regeneration cycles. Primary emphasis during the sulfidation phase will be devoted to determining if H_2S concentrations of 20 ppmv or less can be achieved, and, if so, over what range of conditions. Because of the importance of system cleanliness in achieving low H_2S concentration, the regeneration phase may be omitted in some of these sulfidation tests.

The objective of the regeneration studies will be increase the maximum elemental sulfur concentration from the current 12% to perhaps 20%. From the process analysis effort accompanying the experimental study, it appears that the optimum elemental sulfur concentration should be about 15%. In addition, we will examine the effect of the reaction parameters to provide guidance for additional larger-scale studies in fluidized-bed reactors.